European Journal of Immunology Clinical·Basic·Translational

Adaptive immunity

Basic

Research Article

FURIN regulates cytotoxic T-lymphocyte effector function and memory cell transition in mice

Markus J.T. Ojanen[1], *Fernanda Munoz Caro*[1], *Saara Aittomäki*[1], *Mickaël J. Ploquin*[2], *Zsuzsanna Ortutay*[1], *Meeri Pekkarinen*[1], *Juha Kesseli*[1], *Maria Vähätupa*[1], *Juuso Määttä*[1], *Matti Nykter*[1], *Ilkka S. Junttila*[1,3,4,5], *Tero A.H. Järvinen*[1,6], *John J. O´Shea*[7], *Christine A. Biron*[†2] *and Marko Pesu*[1,3]

[1] Faculty of Medicine and Health Technology, Tampere University, Tampere, Finland
[2] Division of Biology and Medicine, and The Warren Alpert Medical School, Department of Molecular Microbiology and Immunology, Brown University, Providence, RI, USA
[3] Fimlab Laboratories Ltd, Tampere, Finland
[4] Faculty of Medicine, University of Oulu, Oulu, Finland
[5] Department of Clinical Microbiology, Nordlab, Oulu University Hospital, Oulu, Finland
[6] Tampere University Hospital, Tampere, Finland
[7] Lymphocyte Cell Biology Section, Molecular Immunology and Inflammation Branch, National Institute of Arthritis and Musculoskeletal and Skin Diseases, National Institutes of Health, Bethesda, MD, USA

The proprotein convertase subtilisin/kexins (PCSKs) regulate biological actions by cleaving immature substrate proteins. The archetype PCSK, FURIN, promotes the pathogenicity of viruses by proteolytically processing viral proteins. FURIN has also important regulatory functions in both innate and adaptive immune responses but its role in the CD8$^+$ CTLs remains enigmatic. We used a T-cell-specific FURIN deletion *in vivo* to demonstrate that FURIN promotes host response against the CTL-dependent lymphocytic choriomeningitis virus by virtue of restricting viral burden and augmenting interferon gamma (IFNG) production. We also characterized *Furin* KO CD8$^+$ T cells *ex vivo*, including after their activation with FURIN regulating cytokines IL12 or TGFB1. *Furin* KO CD8$^+$ T cells show an inherently activated phenotype characterized by the upregulation of effector genes and increased frequencies of CD44$^+$, TNF$^+$, and IFNG$^+$ cells. In the activated CTLs, FURIN regulates the productions of IL2, TNF, and GZMB and the genes associated with the TGFBR-signaling pathway. FURIN also controls the expression of *Eomes*, *Foxo1*, and *Bcl6* and the levels of ITGAE and CD62L, which implies a role in the development of CTL memory. Collectively, our data suggest that the T-cell expressed FURIN is important for host responses in viral infections, CTL homeostasis/activation, and memory development.

Keywords: FURIN · CD8$^+$ T-cell · LCMV · adaptive immune system · T-cell memory

Additional supporting information may be found online in the Supporting Information section at the end of the article.

Correspondence: Dr. Markus J.T. Ojanen
e-mail: markus.ojanen@tuni.fi

[†]Deceased.

Introduction

The proprotein convertase subtilisin/kexins (PCSKs) are serine endoproteases that activate immature pro-proteins into their functional form by proteolytic cleavage [1, 2]. The conventional members of the PCSK family, namely PCSK1-2, FURIN, and PCSK4-7, cleave their substrate proteins at a (K/R)-(X)n-(K/R)↓ cleavage-motif (X = any amino acid, n = 0, 2, 4 or 6 amino acid residues) [3], and thereby activate a broad array of proteins including growth factors, metalloproteinases, and adhesion molecules [4]. Accordingly, many biological processes including embryogenesis, tissue homeostasis, and malignancies are regulated by the PCSKs [2, 5, 6]. The PCSK family members also cleave bacterial toxins and viral proteins, thus facilitating microbial pathogenicity [6]. In fact, a FURIN-like cleavage site was recently identified on the spike protein of the severe acute respiratory syndrome coronavirus 2 (SARS-CoV-2) [7], and this site was further demonstrated to be critical for viral pathogenesis [8].

In T cells, the expression of *Furin/FURIN* is induced by T-cell receptor (TCR) signaling and interleukin 12 (IL12) and it is consequently upregulated in T helper type 1 (Th1) cells [9, 10]. Critical, nonredundant regulatory functions have been identified for FURIN in both the innate and adaptive immune system. We previously demonstrated that T-cell-expressed FURIN is important for the $CD4^+$ T-cell function, as was indicated by the inherent activation, aberrant polarization of Th cells, and age-related systemic inflammatory disease in *Cd4-Cre-Furin*$^{flox/flox}$ mice with a conditional KO (cKO) of *Furin* in T cells [11, 12]. We have also shown that the lack of FURIN in mouse $LysM^+$ myeloid cells leads to a proinflammatory phenotype characterized by the increased levels of circulating tumor necrosis factor alpha (TNF) and IL6 upon a lipopolysaccharide challenge [13]. Moreover, the immunoregulatory role of FURIN is evolutionarily conserved as deleting *furinA* in the zebrafish (*Danio rerio*) or *Fur1* in the fruit fly (*Drosophila melanogaster*) disrupts normal host responses in bacterial infections [14, 15]. Importantly, the key anti-inflammatory cytokine, transforming growth factor beta-1 (TGFB1), has been shown to upregulate the expression of *FURIN* as well as to be functionally dependent on FURIN-mediated proteolytic maturation [16]. Mechanistically, many of the immunological functions of FURIN are associated with TGFB1 [11], but other FURIN-dependent regulators of the immune response remain currently poorly characterized.

CTLs are important mediators of the immunity against malignant tumor cells and viruses [17, 18]. Recent findings in a mouse model of triple-negative breast cancer (tumor cells lacking estrogen receptor, progesterone receptor, and human epidermal growth factor receptor 2) indicated that the lack of FURIN from T cells reduces tumor growth and the metastatic potential of breast cancer cells, which was attributed to the reduced numbers of tissue-infiltrating regulatory T cells (Tregs) and to an increased infiltration and improved functionality of the $CD8^+$ T cells [19]. In contrast, we have demonstrated a critical role for T-cell-produced FURIN in the immunosurveillance of experimental squamous cell carcinoma in the mouse skin by restricting tumor development [20]. Although FURIN is unequivocally important for the activation of many viral surface proteins, the significance of the FURIN expressed by $CD8^+$ T cells in the host response against viral infections has not been studied.

Here, we used transgenic *Cd4-Cre-Furin*$^{flox/flox}$ mice to study how T-cell-expressed FURIN contributes to the $CD8^+$ T-cell-dependent host response against the lymphocytic choriomeningitis virus (LCMV). In addition, we performed a detailed characterization of *Furin* KO $CD8^+$ T cells *ex vivo*, including after their *in vitro* activation with FURIN regulating cytokines (± IL12 or TGFB1).

Results

Furin cKO mice have high viral titers and low serum IFNG levels in an acute LCMV infection

Using transgenic *Cd4-Cre-Furin*$^{flox/flox}$ mice with a conditional KO of *Furin* in T cells, we have demonstrated that T-cell-expressed FURIN is critical for the $CD4^+FOXP3^+$ T-lymphocyte-dependent immunotolerance and for the polarization of intact Th cells [11, 12, 21]. Previous findings regarding FURIN's role in $CD8^+$ T cells are however controversial as attenuated anti-tumor responses in a DMBA/TPA skin carcinogenesis model [20] and resistance against mammary tumorigenesis [19] have both been attributed to the lack of FURIN in CTLs. To address the significance of FURIN in $CD8^+$ T-cell-mediated immunity, we used an LCMV infection model characterized by CTL-dependent viral clearance [22]. *Cd4-Cre-Furin*$^{flox/flox}$ mice (FURIN absent in both $CD4^+$ and $CD8^+$ T cells) and their *Furin*$^{flox/flox}$ wild type (WT) littermate controls were infected with 2.5×10^4 PFUs of LCMV, and the viral titers were quantified in the spleen at 5 and 8 days post infection (dpi) (Fig. 1A). Here, 8.5-fold higher viral loads were seen in *Cd4-Cre-Furin*$^{flox/flox}$ mice compared to control animals at 5 dpi ($p = 0.004$) with median titers of 88 100 and 10 300 PFUs/spleen, respectively, indicating that the FURIN produced by $CD8^+$ T cells is important in controlling the early LCMV burden. However, both *Cd4-Cre-Furin*$^{flox/flox}$ and *Furin*$^{flox/flox}$ control mice were able to clear the infection as demonstrated by the undetectable LCMV amounts at 8 dpi (data not shown).

A large fraction of the LCMV-specific CTLs secrete interferon gamma (IFNG) that in turn can increase the cytotoxicity of the cells through autocrine signaling [23–25]. We next quantified the concentration of IFNG both in the serum and in the spleen of the LCMV-infected mice and observed significantly lower levels of IFNG in the sera of *Cd4-Cre-Furin*$^{flox/flox}$ animals (355 pg/mL) with a 53% decrease compared to littermate controls (761 pg/mL) ($p = 0.008$) at 5 dpi (Fig. 1B). In contrast, there was no significant difference in the amount of IFNG in the spleens of the mice. Furthermore, the comparable $CD4^+$ and $CD8^+$ T-cell counts between the genotypes (Fig. 1C) suggest that FURIN is not critical for the LCMV-triggered proliferation of T cells *in vivo*. In fact, a trend of higher $CD8^+$ T cell amounts was observed in *Cd4-Cre-Furin*$^{flox/flox}$ mice compared to control animals at 8 dpi (NS, *p*

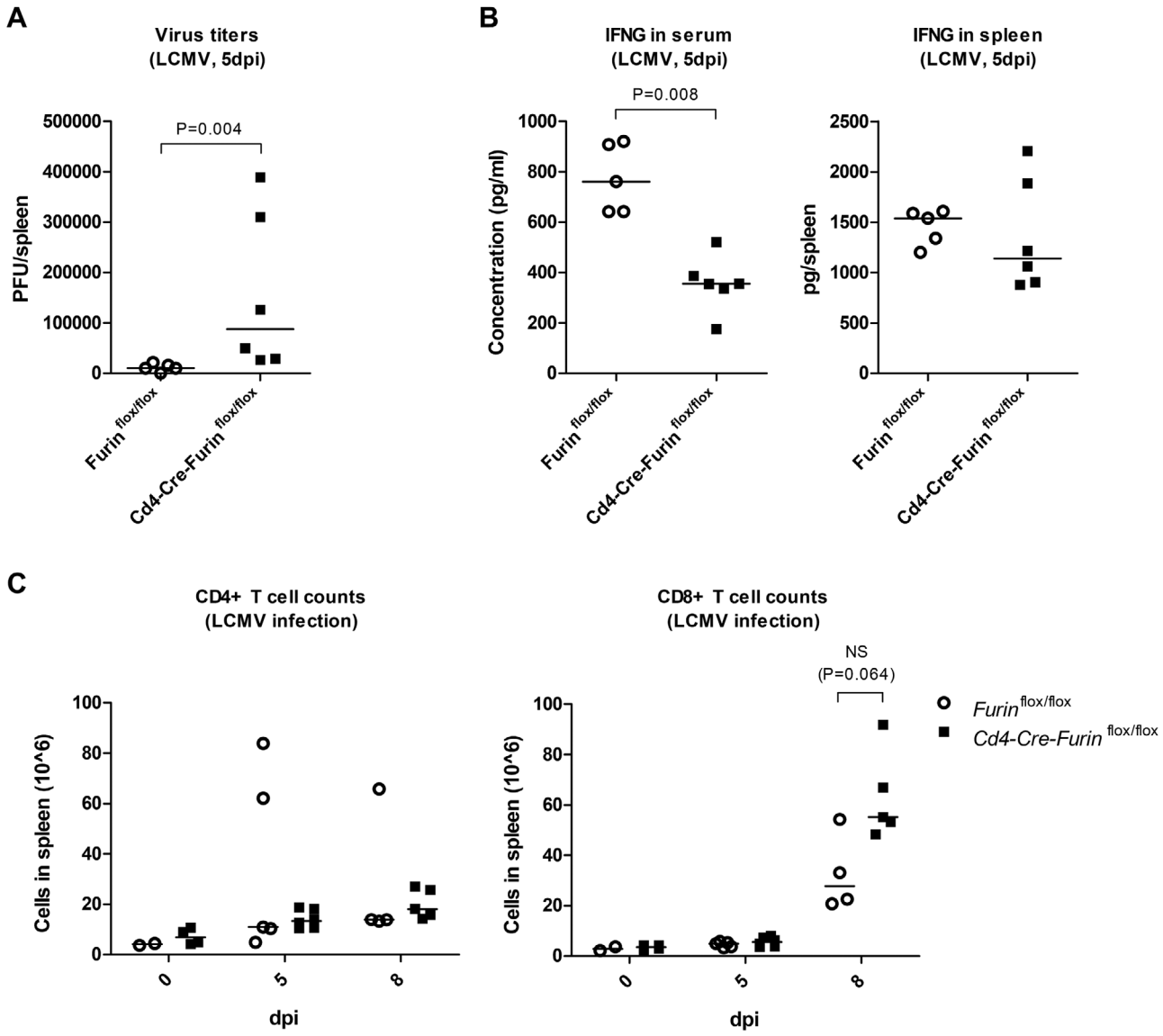

Figure 1. T-cell-expressed FURIN regulates the host response against an LCMV infection in mice. *Cd4-Cre-Furin*$^{flox/flox}$ and *Furin*$^{flox/flox}$ control mice were left untreated (0 dpi) or infected intraperitoneally with LCMV (2.5×10^4 PFU) and the host response was evaluated at 5 and 8 dpi. (A) Viral titers were quantified from the spleen with a standard plaque assay at 5 dpi. (B) IFNG levels were quantified both from the spleen and the serum using ELISA at 5 dpi. (C) Counts of the splenic $CD4^+$ and the $CD8^+$ T cells were determined with flow cytometry at 0, 5, and 8 dpi. Group sizes in *Cd4-Cre-Furin*$^{flox/flox}$ mice were $n = 4$ (three females, one male) at 0 dpi, $n = 6$ (four females, two males) at 5 dpi and $n = 5$ (three females, two males) at 8 dpi, and in *Furin*$^{flox/flox}$ mice $n = 2$ (one female, one male) at 0 dpi, $n = 5$ (three females, two males) at 5 dpi and $n = 4$ (three females, one male) at 8 dpi. Note that 10- to 14-week-old age-matched mice were used in the infections. A representative of two experiments is shown. A two-tailed Mann–Whitney test was used for the statistical comparison of differences.

$= 0.064$). Also, the numbers of NK cells were normal in *Cd4-Cre-Furin*$^{flox/flox}$ mice at 0–6 dpi (data not shown). Collectively, our results indicate that T-cell-produced FURIN is required for an optimal host response against the CTL-dependent pathogen, LCMV.

Lack of FURIN modifies the gene expression profile of naïve $CD8^+$ T cells

To address how FURIN affects the biology of CTLs, we first sorted naïve $CD8^+$ T cells ($CD3^+CD8^+CD62L^+CD44^-$) from the peripheral lymphoid organs of steady-state *Cd4-Cre-Furin*$^{flox/flox}$ and *Furin*$^{flox/flox}$ mice (hereon referred to as *Furin* cKO and WT/control mice, respectively) and performed a genome-wide gene expression analysis by RNA sequencing (Fig. 2). In our post-sorting analyses, a trend of reduced naïve $CD8^+$ T-cell counts was seen in the *Furin* cKO mice compared to the WT controls (NS, $p = 0.051$) (Fig. 2A). A targeted quantification of the aligned reads at the floxed, second exon of the *Furin* gene, demonstrated that the expression of *Furin* was efficiently deleted in the $CD8^+$ T cells of the cKO animals ($p = 0.026$) (Fig. 2B). Furthermore, the absence of FURIN in the $CD8^+$ T cells affected the expression of

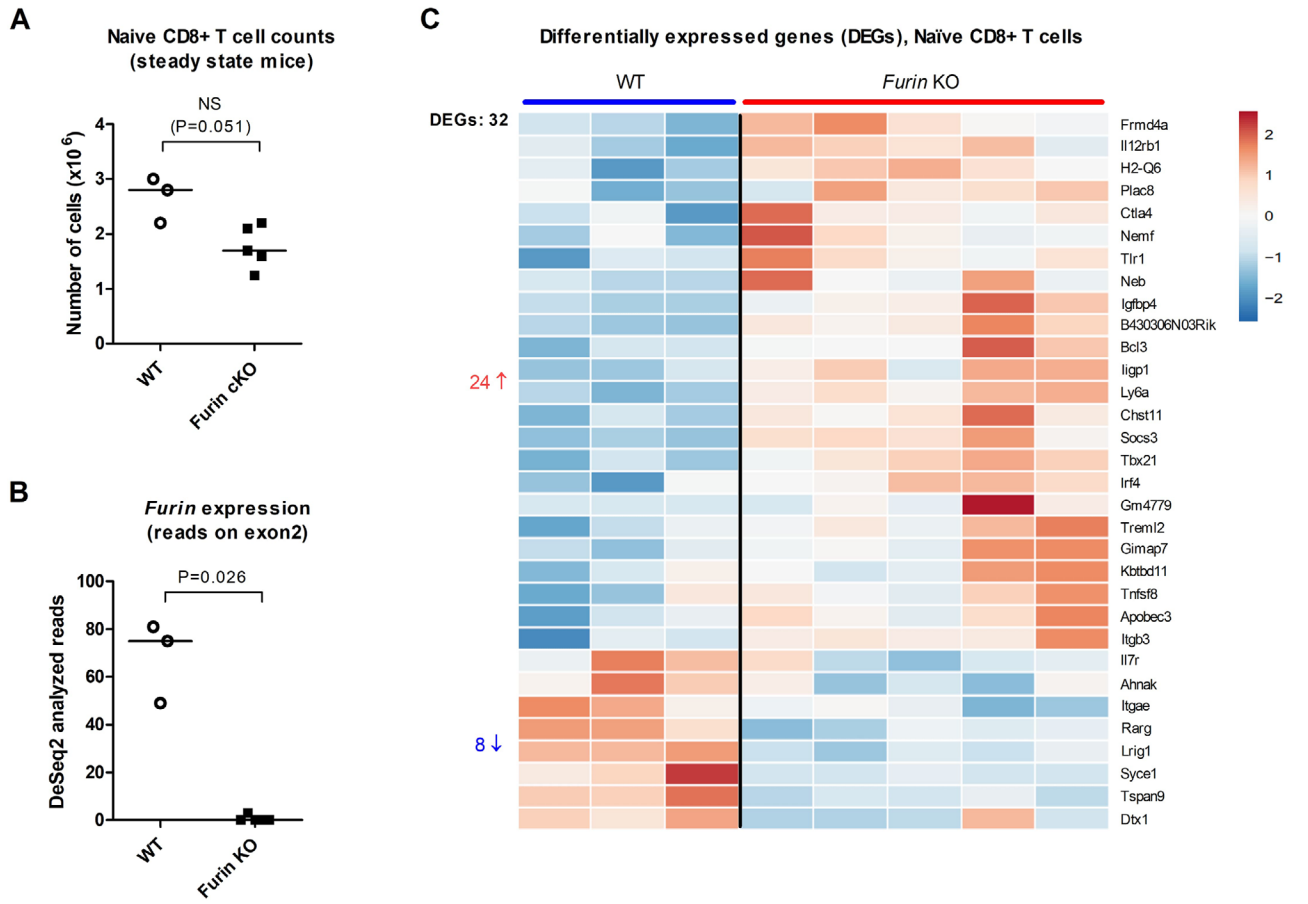

Figure 2. The absence of FURIN in naïve CD8$^+$ T cells upregulates genes associated with T-cell activation. The naïve CD8$^+$ T cells were enriched and sorted from the LNs and spleen of 8- to 9-week-old steady-state *Furin* cKO ($n = 5$, all males) and WT mice ($n = 3$, all males) followed by a genome-wide gene expression analysis using RNA sequencing. (A) The naïve CD8$^+$ T-cell counts were quantified with FACS. (B) The expression of *Furin* was evaluated from the floxed, second exon region of *Furin* mRNA using a targeted analysis of the aligned reads at this site. (C) Differentially expressed genes (DEGs) between the genotypes were determined using DESeq2 and are depicted using a heatmap normalized to an interval between −2 and 2. Blue represents low and orange high gene expression levels. A two-tailed Mann–Whitney test was used for the statistical comparison of differences in panel (A), whereas in panels (B) and (C) the DESeq2 statistics adjusted using the Benjamini–Hochberg method were applied.

32 protein-coding genes (24 upregulated and 8 downregulated) compared to control cells (adjusted $p < 0.05$) (Fig. 2C). Specifically, we detected higher expression levels of T-cell transcription factor genes, such as *t-box transcription factor 21* (*Tbx21*, 3.80-fold change, $p = 0.005$) and *interferon regulatory factor 4* (*Irf4*, 3.12-fold change, $p = 0.020$), and of genes related to T-cell activation, such as *il12 receptor subunit beta 1* (*Il12rb1*, 1.97-fold change, $p = 0.019$) and *suppressor of cytokine signaling 3* (*Socs3*, 1.87-fold change, $p < 0.001$) in the naïve *Furin* KO CD8$^+$ T cells compared to controls. In addition, the immune checkpoint receptor gene *cytotoxic T-lymphocyte associated protein 4* (*Ctla4*) was upregulated (2.20-fold change, $p = 0.035$) in the absence of FURIN. Conversely, genes including *Il7r* (0.77-fold change, $p = 0.013$) and *integrin subunit alpha E* (*Itgae*, 0.76-fold change, $p < 0.001$) were downregulated in the naïve *Furin* KO CD8$^+$ T cells.

We have previously shown that the thymic development of single-positive (SP) CD4$^+$ and CD8$^+$ T cells as well as the negative selection of Th cells are intact in *Cd4-Cre-Furin*$^{flox/flox}$ mice [11]. In contrast, the numbers of thymic CD4$^+$FOXP3$^+$ T cells in *Furin* cKO animals were increased compared to littermate controls [11]. To elucidate whether FURIN-deficient SP CD8$^+$ T cells in the thymus are inherently activated, we determined the frequencies of CD8$^+$FOXP3$^+$, CD8$^+$IL2RA$^+$, and CD8$^+$CD44$^+$ cells in *Furin* cKO and littermate mice (Supporting information Fig. S1). Here, the FURIN deficiency did not affect the proportions of FOXP3 (1.1% in WT and 1.0% in *Furin* cKO mice), IL2RA (5.1% and 5.5%), or CD44 (9.8% and 9.2%) positive SP CD8$^+$ T cells in the thymus. Our analyses suggest that the lack of FURIN promotes the T-cell effector phenotype in peripheral naïve CD8$^+$ T lymphocytes, but the T-cell activation is not evident during thymic T-cell development.

Steady state *Furin* cKO mice have an activated CD8$^+$ T-cell phenotype

While the elevated early LCMV burden in *Furin* cKO mice may be attributed to the reduced IFNG, other factors, such as different

cytokines and the function of $CD4^+$ T lymphocytes, are likely to affect the response. For example, the previously reported autoimmune phenotype in aging *Furin* cKO mice [11] could be causing a dysregulation of the immune system in LCMV-infected *Furin* cKOs. To understand how the $CD8^+$ T-cell subsets are affected by the absence of FURIN and aging, we used flow cytometry to phenotype $CD8^+$ T cells from the spleen and LNs of steady-state *Furin* cKO mice and their WT littermates at the age of 3 (prior to auto-immunity) and 5 months (at the onset of auto-immunity) (Fig. 3). In our *ex vivo* characterization, we did not detect any significant difference in the numbers of $CD8^+$ T cells between the genotypes in the 3-month-old animals or in the splenic $CD8^+$ T lymphocyte counts of 5-month-old mice (Fig. 3B). However, a trend of higher $CD8^+$ T-cell numbers was observed in the LNs of 5-month-old *Furin* cKO mice compared to the WT controls (NS, $p = 0.057$). In contrast, the frequency of $CD8^+$ T lymphocytes was lower both in the spleen (3-month-old: NS, P = 0.057 and 5-month-old: $p = 0.029$) and LNs ($p = 0.029$ in both age groups) of the *Furin* cKO mice (Supporting information Fig. S2).

Next, we analyzed the splenic $CD8^+$ T cells for the expression of the T-cell activation/exhaustion markers CD44, CD69, programmed cell death protein 1 (PD1), and IL7RA (Fig. 3C and D). This approach revealed comparable average frequencies of $CD44^+$ (32.7% in WT and 41.3% in *Furin* cKO mice), $CD69^+$ (10.3% and 12.2%) and $PD1^+$ (8.6% and 9.2%) cells, but a lower frequency of $IL7RA^+$ cells (88.1% and 78.8%, $p = 0.029$) in the 3-month-old *Furin* cKO mice. A flow cytometry analysis of the spleen cells of 5-month-old animals demonstrated that significantly higher fractions of $CD8^+$ T cells were positive for CD44 (29.5% and 60.7%, $p = 0.029$) and CD69 (7.7% and 13.8%, $p = 0.029$) in the *Furin* cKO mice compared to WT animals, whereas the frequencies of $PD1^+$ cells were not substantially affected by the genotype or by aging. The splenic $IL7RA^+$ population of $CD8^+$ T cells was smaller in the absence of FURIN also in 5-month-old mice (94.7% and 77.6%, $p = 0.029$). Furthermore, when we used the same surface markers to phenotype the $CD8^+$ T cells from the LNs, we correspondingly identified higher frequencies of cells that were positive for CD44 (3-month-old mice: 33.1% and 40.6%, 5-month-old mice: 37.3% and 43.1%, $p = 0.029$ in both comparisons) as well as a decrease in the frequencies of $IL7RA^+$ cells (5-month-old mice: 92.7% and 81.9%, $p = 0.029$) in *Furin* cKO mice compared to controls (Supporting information Fig. S2B). Interestingly, a decrease in the percentage of the $PD1^+$ population was observed in the LNs of FURIN-deficient animals at 5 months of age (22.1% and 13.5%, $p = 0.029$) (Supporting information Fig. S2B).

In order to assess the role of FURIN in the production of effector proteins in the $CD8^+$ T cells, we next performed a flow cytometric analysis for perforin-1 (PRF1), Fas ligand (FASL), TNF, and IFNG in the steady-state *Furin* cKO mice and the littermate controls (Fig. 3E and F, Supporting information Fig. S2C). We did not detect differences in the frequencies of $PRF1^+$ (spleen: 35.0% and 38.5%, LNs: 44.8% and 46.1%), $FASL^+$ (spleen: 27.6% and 30.4%, LNs: 13.6% and 16.7%), or TNF^+ (spleen: 35.3% and 48.9%, LNs: 44.4% and 48.4%) CTLs of the younger 3-month-old animals (Fig. 3E and F). The amount of $IFNG^+CD8^+$ T cells was in turn increased in the spleen of 3-month-old *Furin* cKO mice compared to WT animals (26.4% and 45.0%, $p = 0.029$). In the 5-month-old mouse spleens, the frequencies of cells positive for PRF1 (53.1% and 54.5%) and FASL (27.0% and 27.9%) were comparable between the genotypes, whereas more of both TNF (37.8% and 69.0%, $p = 0.029$) and IFNG producing $CD8^+$ T cells (36.5% and 76.3%, $p = 0.029$) were detected in the *Furin* cKO mice (Fig. 3E and F). Moreover, CD8+ T cells isolated from the LNs of these animals revealed a higher $FASL^+$ cell frequency (17.1% and 28.0%, $p = 0.029$) in the absence of FURIN (Supporting information Fig. S2C). Noteworthy, the frequencies of the $CD107a^+$ (CTL degranulation marker) cells were comparable between the genotypes in both 3- and 5-month-old mice (data not shown). An additional analysis of the mean fluorescence intensity (MFI) revealed that the $CD8^+$ T cells from the 3-month-old *Furin* cKO mice expressed more TNF in the spleen ($p = 0.029$) and more IFNG in both LNs and in the spleen compared to WT controls ($p = 0.029$ in both comparisons) (Supporting Information Fig. S2D), and that the MFIs of PRF1 (in LNs and in the spleen, $p = 0.029$ in both comparisons), TNF (in the spleen, $p = 0.029$), and IFNG (in LNs and spleen, $p = 0.029$ in both comparisons) positive CTLs were higher in the *Furin* cKO mice at 5 months of age (Supporting information Fig. S2E). In conclusion, our data indicate that FURIN restrains the activation of $CD8^+$ T cells in steady-state mice and that the inherent activation phenotype in *Furin* KO $CD8^+$ T cells is associated with an elevated production of effector proteins and pronounced in aging animals.

In vitro stimulation of *Furin* KO $CD8^+$ T cells alters the secretion of IL2, GZMB, and TNF

We next evaluated how FURIN affects the production of the effector proteins in the *ex vivo* activated $CD8^+$ T cells in different culture conditions. To this end, we stimulated naïve $CD8^+$ T cells from steady-state *Furin* cKO and WT mice *in vitro* for 3 days using plate-bound anti-CD3 and anti-CD28 antibodies and quantified the concentrations of IL2, granzyme B (GZMB), TNF, and IFNG in the culture media (Fig. 4). To simultaneously assess how the absence of FURIN is affected by IL12 and TGFB1, both known regulators of *Furin/FURIN* expression [9, 10, 16], these cytokines were included in the experimental setup. We used serum-free culture conditions, which enabled us to specifically determine the significance of TGFB1 produced by $CD8^+$ T cells and its autocrine effects. Importantly, as FURIN is critical for the proteolytic maturation and bioavailability of TGFB1 [11, 16], the aforementioned setup also allowed us to evaluate whether the lack of FURIN can be compensated for by adding exogenous, active TGFB1. The administration of IL12 expectedly induced the production of the proinflammatory factors GZMB ($p = 0.008$), TNF ($p = 0.032$), and IFNG ($p = 0.008$) in the WT cells (Fig. 4B). In the presence of TGFB1, the secretion of IL2 ($p = 0.016$) was decreased and the GZMB production abolished (Mann–Whitney analysis not applicable). Our results also demonstrated that the stimulated

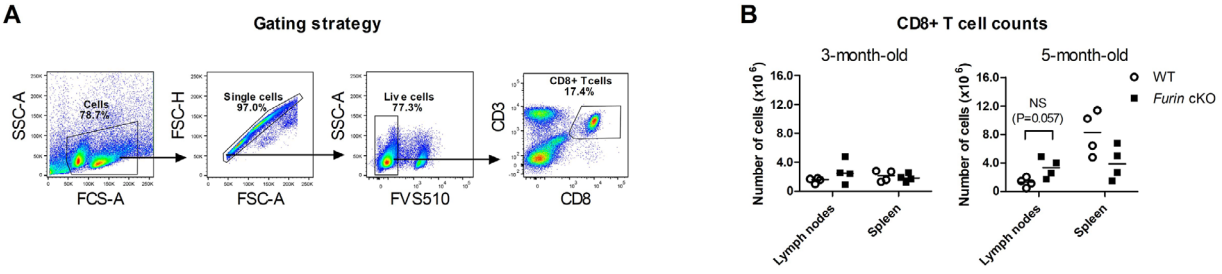

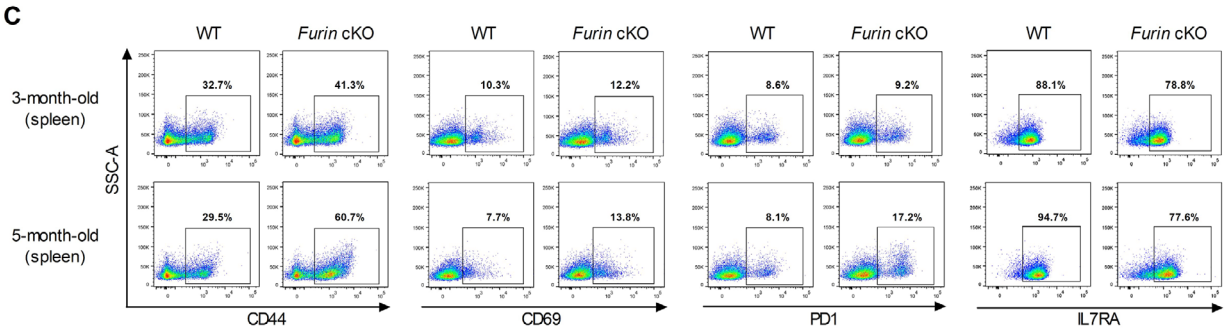

D

3-month-old (spleen)

	WT				Furin cKO			
CD44	1.03	0.95	0.68	0.97	1.33	1.30	0.92	1.08
CD69	0.73	0.90	0.92	1.10	1.17	1.08	0.90	1.10
PD1	0.61	1.03	0.83	1.15	0.83	1.08	0.97	1.11
IL7RA* (P=0.029)	1.10	1.01	1.06	1.07	0.93	0.92	0.99	0.95

5-month-old (spleen)

	WT				Furin cKO			
CD44* (P=0.029)	0.61	0.57	0.71	0.73	1.33	1.54	1.30	1.27
CD69* (P=0.029)	0.64	0.60	0.72	0.87	1.14	1.32	1.28	1.13
PD1	0.71	0.62	0.99	1.01	0.95	3.57	1.36	1.21
IL7RA* (P=0.029)	1.07	1.08	1.07	1.05	0.95	0.79	0.84	0.92

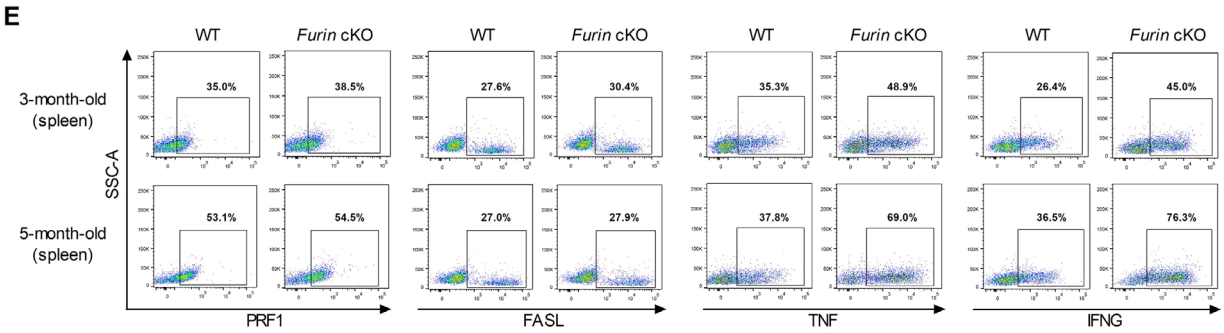

F

3-month-old (spleen)

	WT				Furin cKO			
PRF1	0.95	1.02	0.94	0.98	1.21	1.05	0.91	1.10
FASL	0.48	0.90	1.03	1.02	0.45	0.98	1.17	1.13
TNF	1.05	0.85	0.70	0.81	1.28	1.23	0.95	1.26
IFNG* (P=0.029)	0.94	0.95	0.71	0.84	2.05	1.40	1.05	1.41

5-month-old (spleen)

	WT				Furin cKO			
PRF1	0.88	1.03	1.00	0.98	0.87	1.01	1.00	1.12
FASL	0.88	0.74	1.06	1.30	1.13	0.94	0.91	1.10
TNF* (P=0.029)	0.64	0.79	0.73	0.70	1.21	1.41	1.35	1.34
IFNG* (P=0.029)	0.75	0.66	0.64	0.71	1.25	1.64	1.54	1.34

Figure 3. *Furin* cKO mice have overtly activated splenic CD8$^+$ T cells compared to control animals. Flow cytometry was used to assess the CD8$^+$ T-cell counts and the activation/effector status of these cells in 3- and 5-month-old *Furin* cKO and WT mice ($n = 4$ in all experimental groups; two females, two males). (A) A representative gating strategy used for the phenotyping of the CD8$^+$ T cells. (B) The total cell counts in the lymph nodes and spleen were calculated and concomitantly compared to the relative frequencies of the CD8$^+$ T cells from the flow cytometric analysis to determine the total CD8$^+$ T-cell numbers in each mouse. (C and E) The target populations were gated based on the granularity (SSC-A) and the expression of CD44, CD69, PD1, IL7RA, PRF1, FASL, TNF, and IFNG, and the representative flow cytometry plots within the splenic CD8$^+$ T-cell compartment are shown. Gates demonstrate the average frequency of a population within a group. (D and F) Frequencies of the splenic CD8$^+$ T cells positive for CD44, CD69, PD1, IL7RA, PRF1, FASL, TNF, and IFNG in each mouse were normalized to the average frequency of the same marker within the corresponding age group and the relative color-coded expression values are shown. In panels (C) and (E), 1000–5000 down-sampled cells were used from each sample and the concatenated FCS-files (4000–20 000 cells/genotype) are depicted. In panels (D) and (F), the protein expression was normalized to an interval between 0 and 3 in which blue represents a low and red a high relative abundancy of a given protein. The flow cytometric analyses for the 3- and the 5-month-old mice were performed once as separate experiments. A two-tailed Mann–Whitney test was used for the statistical comparison of differences.

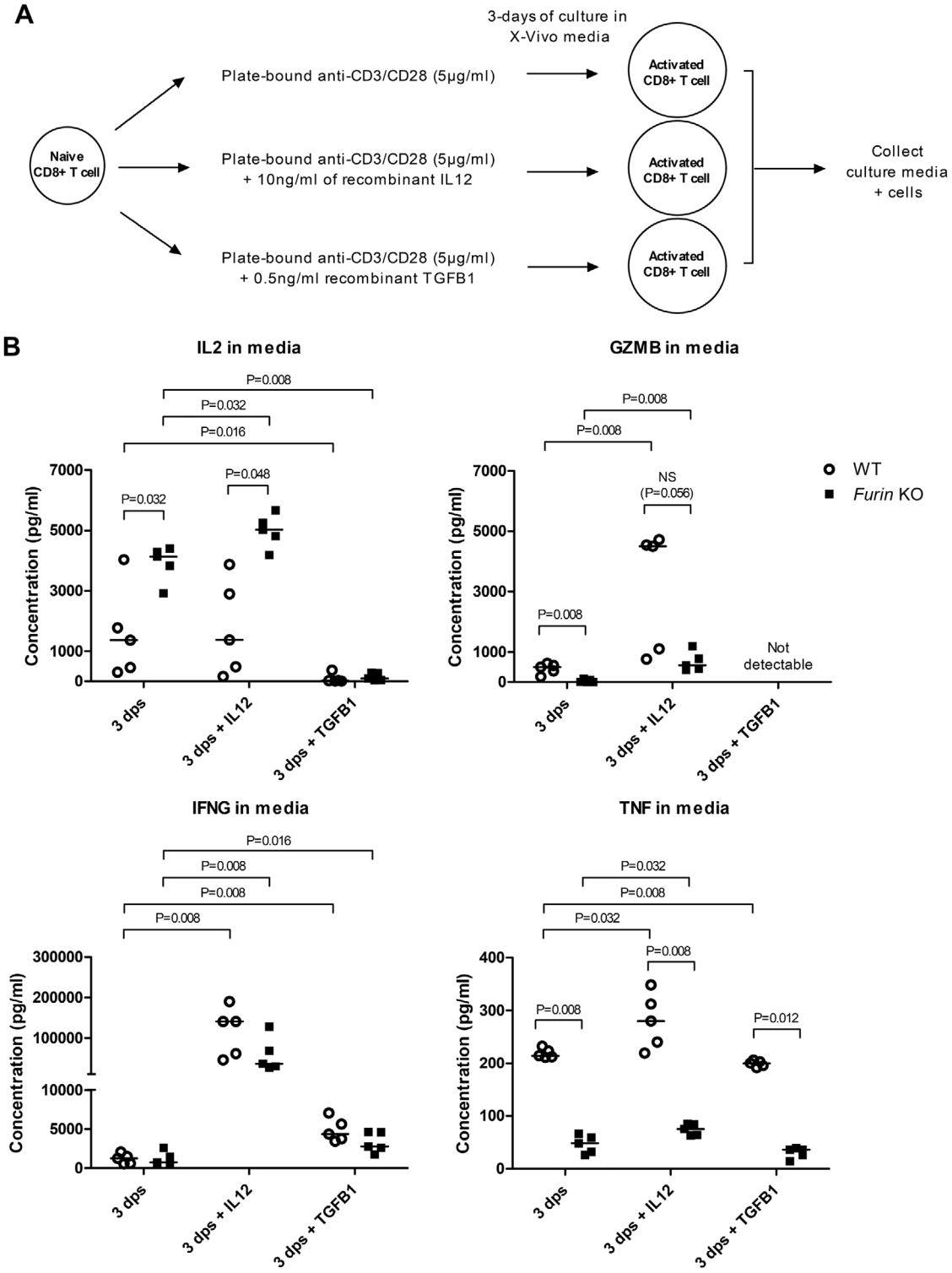

Figure 4. FURIN restricts IL2 and augments GZMB and TNF production in CD8$^+$ T cells upon TCR-mediated *in vitro* stimulation. (A) A schematic representation of the experimental set up is shown. Naïve CD8$^+$ T cells were isolated from 9-week-old *Furin* cKO ($n = 5$, four females, one male) and WT mice ($n = 5$, four females, one male) and 470 000–1 200 000 cells were stimulated *in vitro* for 3 days in serum-free media. Plate-bound anti-CD3 and anti-CD28 antibodies (5 µg/mL of both) or the antibodies together with either recombinant IL12 (10 ng/mL) or TGFB1 (0.5 ng/mL) were used. Both cells and culture media were collected for a further analysis. (B) IL2, GZMB, IFNG, and TNF concentrations were quantified from the culture media using ELISA. ELISA was performed a minimum of two times as technical duplicates to achieve the optimal concentration of the target protein for the analysis. A two-tailed Mann–Whitney test was used for the statistical comparison of differences.

FURIN-deficient CTLs could similarly respond to IL12 by producing significantly more GZMB ($p = 0.008$), TNF ($p = 0.032$), and IFNG ($p = 0.008$) in comparison to corresponding cells not receiving cytokines. Additionally, the response to exogenous TGFB1 was recapitulated in *Furin* KO CTLs as indicated by the marked decrease in IL2 ($p = 0.008$) and GZMB levels (Mann–Whitney analysis not applicable). Without added cytokines, the lack of FURIN from the $CD8^+$ T cells was associated with the increased production of IL2 in comparison to WT cells ($p = 0.032$), whereas the levels of GZMB ($p = 0.008$) and TNF ($p = 0.008$) were significantly decreased at 3 dps. The production of IFNG was not altered between the *Furin* KO and the control cells. Further comparisons between the *Furin* KO and control CTLs demonstrated that in the presence of added cytokines the FURIN-deficient cells expressed more IL2 (IL12-treated cells, $p = 0.048$) and they had substantially lower levels of TNF (IL12- and TGFB1-treated cells, $p = 0.008$ and $p = 0.012$, respectively) than the controls.

To investigate the possibility that FURIN deletion in other T-cell subtypes, such as $CD4^+$ T or natural killer T (NKT) cells, *in vivo* could underly the observed *Furin* KO CTL phenotype, we used naïve $CD8^+$ T cells from WT C57BL/6JRj mice and treated them with FURIN/PCSK-inhibitor (CMK) [26, 27]. The FURIN-dependent production of effector proteins seen in *Furin* KO CTLs from *Cd4-Cre-Furin*$^{flox/flox}$ mice was partially recapitulated at a 10 μM CMK concentration as attested by significantly reduced TNF production and higher IL2 and lower GZMB level medians (Supporting information Fig. S3). Interestingly, a higher concentration of CMK (30 μM) completely abolished T-cell activation, which could be indicative of the role of other PCSKs in T-cell activation or unspecific inhibition of other T-cell activation-associated proteases. Collectively, the cytokine quantifications in the TCR/cytokine activated $CD8^+$ T cells suggest that the lack of FURIN inherently augments IL2 production and impairs the secretion of effector proteins GZMB and TNF in activated CTLs. However, the FURIN-deficient cells are able to respond to both of the cytokines that regulate *Furin* expression, IL12 and TGFB1. Importantly, ectopic TGFB1 cannot fully compensate for the effects caused by the lack of FURIN from the $CD8^+$ T cells, since TNF production remains lower also in the presence of TGFB1. This clearly argues for the presence of FURIN-dependent and TGFB1-independent effects in the TCR-activated $CD8^+$ T cells.

IL12- and TGFB1-mediated transcriptomic response in activated *Furin* KO CTLs

We next assessed the genome-wide transcriptomic response of the *in vitro* stimulated *Furin* KO and control $CD8^+$ T cells (see Fig. 4A). RNA sequencing revealed that upon TCR stimulation the absence of FURIN influenced the expression of a large number of genes compared to the control cells; 452 differentially expressed genes (DEGs, adjusted $p < 0.05$) without added cytokines (hereon referred to as the 3 dps group, 222 up- and 230 downregulated in FURIN-deficient $CD8^+$ T cells), 1036 DEGs with IL12 (3 dps + IL12 group, 448 upregulated and 588 downregulated) and 4224 DEGs with TGFB1 (3 dps + TGFB1 group, 2214 upregulated and 2010 downregulated) (Fig. 5A). The number of DEGs thus became clearly upregulated when IL12 or TGFB1 was added to the culture with 571 and 3763 treatment-specific DEGs, respectively, versus 147 DEGs specific for the 3 dps group (Fig. 5B). Within the treatment-specific transcripts, the 3 dps group showed a marked increase in the expression of genes including *programmed cell death protein 1* (*Pdcd1*, better known as *Pd1*) and *nitric oxide synthase, inducible* (*Nos2*) as well as the downregulation of *Il10ra* and *Il7r* in the *Furin* KO cells. In the 3 dps + IL12 group, *Cd28* and *Cd81* were specifically upregulated, whereas *Il10* and *immunity-related GTPase family M member 2* (*Irgm2)* were downregulated in the absence of FURIN. Furthermore, the *Furin* KO cells had increased expression of genes such as *Il2* and *Cd44* and reduction in the mRNA levels of *signal transducer and activatior of transcription 2* (*Stat2)* and *Cd2* in both of the immunostimulatory conditions: the 3 dps and the 3 dps + IL12 groups. An analysis of the 3 dps + TGFB1 group demonstrated that in the *Furin* KO cells TGFB1 leads to specific upregulation of *Il9* and *Il2ra* and downregulates genes such as *MX dynamin-like GTPase 1* (*Mx1)* and *Gzmb*. Finally, in all experimental groups, we observed differential expression of genes such as *Cd9*, *a disintegrin and metallopeptidase domain 15* (*Adam15)*, *chemokine* (*C-X-C motif) receptor 5 (Cxcr5*), and *Il2rb* in the *Furin* KO CTLs, suggesting that the expression of these FURIN-dependent genes is independent of IL12 or TGFB1 administration.

In agreement with the ELISA data, the principal component analysis demonstrated that both IL12 and TGFB1 were able to modify the gene expression profile in both genotypes (Supporting information Fig. S4). In fact, when we specifically analyzed how IL12 and TGFB1 affected the transcriptome of the TCR-activated $CD8^+$ T cells, we identified 2318 (*Furin* KO cells) and 1845 DEGs (control cells) between 3 dps and 3 dps + IL12 groups, respectively, whereas a similar evaluation of the 3 dps versus 3 dps + TGFB1 groups revealed 3470 and 3856 DEGs (Fig. 5C). We could also see that only 39.0% (1169) of the IL12-responsive and 29.2% (1657) of the TGFB1-responsive genes were common for both FURIN-deficient and control cells. These results suggest that the transcriptomic response to IL12 and TGFB1 is only partially preserved in stimulated *Furin* KO $CD8^+$ T cells. To conclude, in activated CTLs the lack of FURIN affected the expression of more than 400 genes, and in the presence of the pro-inflammatory cytokine IL12 the number of FURIN-dependent transcripts was higher than in its absence. However, the most pronounced effects on gene expression in stimulated *Furin* KO $CD8^+$ T cells compared to the control cells were seen by adding anti-inflammatory TGFB1, which may be indicative of the critical role of FURIN in TGFB1-dependent tolerogenic responses.

To gain additional insights on how the absence of FURIN impacts the transcriptome of $CD8^+$ T cells upon TCR stimulation, we performed gene ontology (GO) enrichment analysis using GOrilla [28] (Supporting information Table S1). GO analysis of the upregulated genes in the *Furin* KO $CD8^+$ T cells without added cytokines (the 3 dps group) revealed enrichment of several immunological processes such as regulation of cytokine

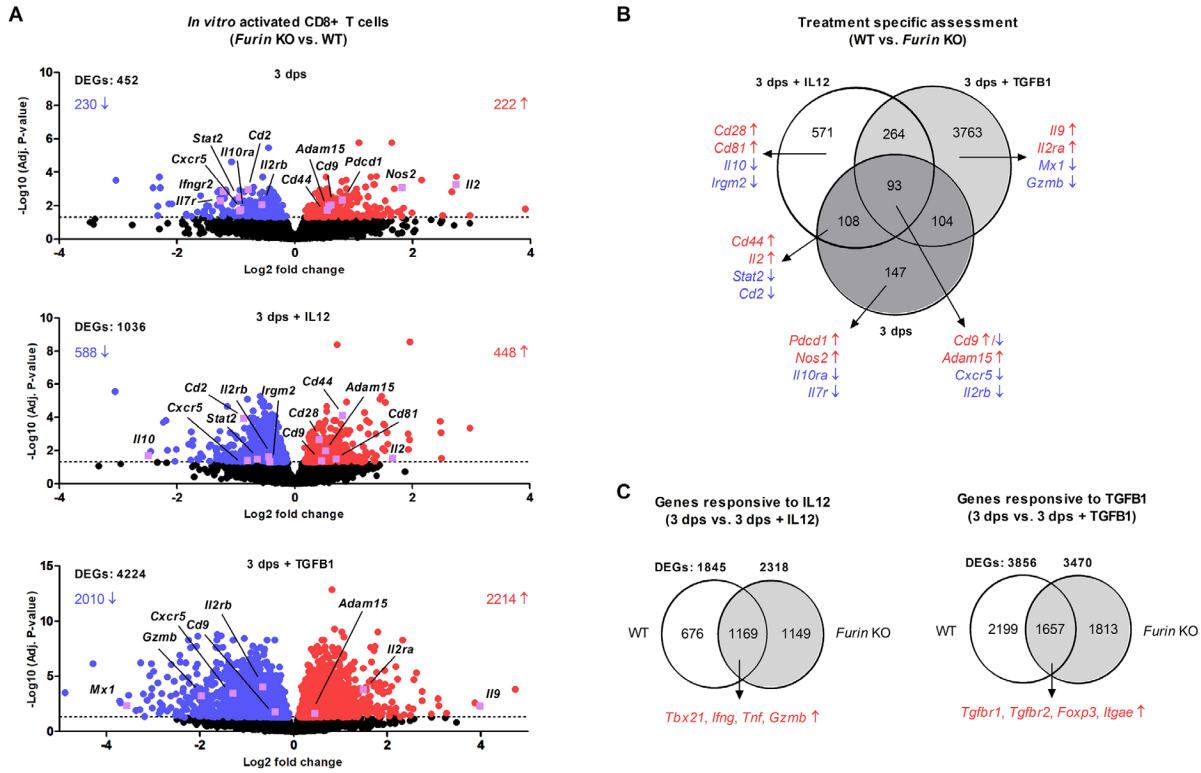

Figure 5. Genome-wide expression analyses of *in vitro* activated FURIN-deficient and WT CD8$^+$ T cells. Total RNA was isolated from the *in vitro* stimulated CD8$^+$ T cells, and a genome-wide gene expression analysis was performed using RNA sequencing. (A) Genes expressed differentially between *Furin* KO and WT cells were analyzed using DESeq2 and are depicted using volcano plots. Down- and upregulated genes in *Furin* KO cells are shown as blue and red, respectively, and genes of interest (purple) are highlighted. Dashed line indicates the adjusted *p*-value threshold of 0.05. (B) Venn diagram showing the counts of both treatment specific as well as common DEGs between *Furin* KO and WT CD8$^+$ T cells. Examples of genes upregulated (red ↑) or downregulated (blue ↓) in the *Furin* KO cells are also shown. (C) DEGs without added cytokines were compared to the IL12- and TGFB1-treated cells separately in *Furin* KO and in control cells using DESeq2. Venn diagrams were then compiled to determine the specific and common genes responsive to the cytokines in *Furin* KO and in control cells. Examples of upregulated (red ↑) genes in both genotypes are additionally shown. The experiment was performed once. Statistical evaluation of differences was done using DESeq2 and adjusted using the Benjamini–Hochberg method.

production (GO:0001817), immune system process (GO:0002376), and monocyte chemotaxis (GO:0002548), whereas GO terms including response to virus (GO:0009615), defense response to virus (GO:0051607), and immune effector process (GO:0002252) were enriched among the downregulated genes. In the 3 dps + IL12 group, the upregulated genes were enriched with processes such as cell adhesion (GO:0007155), regulation of signaling (GO:0023051), and regulation of cell communication (GO:0010646), whereas the 3 dps + TGFB1 group revealed several metabolic (e.g., cellular metabolic process: GO:0044237 and ncRNA metabolic process: GO:0034470) and biosynthetic GO-terms (e.g., cellular component biogenesis: GO:0044085 and organonitrogen compound biosynthetic process: GO:1901566). Interestingly, GO terms such as, defense response to other organism (GO:0098542) and response to virus (GO:0009615) were also pronounced within the downregulated genes of the TGFB1-treated *Furin* KO CD8$^+$ T cells. More specifically, within the GO term, response to virus (GO:0009615), we identified 10 downregulated genes (*Bcl3*, *Ddit4*, *Dhx58*, *Ifit3*, *Il10rb*, *Irf1*, *Isg15*, *Lgals9*, *Parp9*, and *Zbp1*) that were common for all three experimental groups (3 dps, 3 dps + IL12, and 3 dps + TFGB1). In conclusion, our transcriptomic data suggest that the absence of FURIN from the CD8$^+$ T cells can lead to an attenuated anti-viral transcriptomic response, providing further understanding to our results obtained from the LCMV-infected *Cd4-Cre-Furin*$^{flox/flox}$ mice.

FURIN regulates the TGFB gene signature and promotes memory cell transition in CD8$^+$ T cells

Many of the immunobiological functions of FURIN can be directly attributed to the nonredundant role of FURIN in the processing of pro-TGFB1 [11, 13]. Theoretically, the observed transcriptomic differences in the *in vitro* stimulated *Furin* KO CD8$^+$ T cells could thus arise from the deficient production of mature TGFB1 and the subsequent dysfunctionality of its autocrine signaling. However, the increased number of DEGs between the *Furin* KO and the control cells in the 3 dps + TGFB1 condition indicates that adding TGFB1 to the culture media does not normalize gene expression but enhances the difference in transcription. To understand whether this could be explained by a differential

expression of the TGFB1 signature genes, we first compared the expression of *Tgfb1*, *Tgfbr1*, *Tgfbr2*, *SMAD family member 2 (Smad2)*, *Smad3*, *Smad4*, *Smad7*, *Itgae*, and *Foxp3* in the *in vitro* activated *Furin* KO and the WT CTLs in the presence of ectopic TGFB1 (Fig. 6A). Importantly, we identified the upregulation of *Tgfb1* (1.27-fold change, $p = 0.006$), *Smad2* (1.48-fold change, $p < 0.001$), and *Foxp3* (3.57-fold change, $p < 0.001$) in *Furin* KO cells, whereas the transcript levels of *Tgfbr2* (0.45-fold change, $p < 0.001$), *Smad3* (0.59-fold change, $p = 0.039$), *Smad7* (0.49-fold change, $p = 0.003$), and *Itgae* (0.17-fold change, $p < 0.001$) were significantly decreased in the absence of FURIN. In contrast, the expressions of *Tgfbr1* and *Smad4* remained unaffected by the genotype of the cells. Additionally, we performed PCSK-cleavage site analysis of TGFB-signaling pathway components using ProP 1.0 [29] (Supporting information Table S2). Here, we expectedly identified previously reported PCSK cleavage sites for TGFB1, ITGAE, and FOXP3 [11, 30, 31]. Interestingly, our analysis indicated that also TGFBR1 and SMAD7 contain canonical FURIN-type cleavage site sequences (R-X-X-R-↓). Collectively, our data reveal that the expression of several components of the TGFB1 signaling pathway, as well as its target genes, are altered in the $CD8^+$ T cells lacking FURIN, and that both verified and potential FURIN cleavage sites are present on several TGFB1 signature proteins.

Previously TGFB1 signaling through TGFBR2 has been shown to intrinsically regulate the differentiation and maintenance of memory $CD8^+$ T cells [32]. ITGAE (also known as CD103) is a TGFBR-SMAD2/3-regulated integrin expressed on intraepithelial lymphocytes and on tumor infiltrating $CD8^+$ T lymphocytes (TILs), and it is used as a marker for tissue resident memory T cells (T_{RM}) [33, 34]. In line with the lower *Itgae* gene expression in naïve and in *in vitro*-activated $CD8^+$ T cells lacking FURIN (Figs. 2C and 6A), we detected a reduced frequency of $CD8^+$ T cells positive for cell surface ITGAE in the LNs and spleen of steady-state *Furin* cKO mice (43.3% and 32.7%, respectively) compared to the controls (65.2% and 53.1%, respectively) ($p = 0.029$ in both comparisons) (Fig. 6B). However, although ITGAE promotes the retention of $CD8^+$ T cells in the tissues contributing to the host response against viral infections and tumor cells [35], we did not detect any difference between the genotypes in the number of $CD8^+$ cells in the skin or in the dermis underneath papillomas in untreated mice or after 17 weeks of DMBA/TPA treatment (Supporting information Fig. 5A and B). Instead, we observed downregulation of several genes that have previously been associated with the effector to memory transition of CTLs [36], when FURIN KO $CD8^+$ T cells were activated in the presence of TGFB1: *eomesodermin* (*Eomes,* 0.49-fold change, $p < 0.001$), *forkhead box O1* (*Foxo1*, 0.72-fold change, $p = 0.004$), B cell CLL/lymphoma 6 (*Bcl6,* 0.15-fold change, $p < 0.001$), *transcription factor 7, T-cell specific* (*Tcf7,* 0.49-fold change, $p = 0.009$), and *inhibitor of DNA binding 3* (*Id3,* 0.27-fold change, $p < 0.001$) (Fig. 6C).

To further examine whether the lack of FURIN in the $CD8^+$ T cells could affect the memory lymphocyte populations, we next analyzed the expression of CD3, CD8, CD44, and CD62L in the peripheral lymphoid organs of *Furin* cKO and WT mice using flow cytometry. A comparison of the central memory ($CD62L^+CD44^+$) and effector/effector memory (Eff./EM; $CD62L^-CD44^+$) populations of $CD8^+$ T cells revealed a differentiating pattern of expression for CD62L in the absence of FURIN (Fig. 6D). In fact, while the WT animals showed a distinguishable separation between the central memory and the Eff./EM subsets in both LNs and the spleen, the *Furin* cKO mice had an additional "intermediate" population with moderate CD62L expression as well as a clearly distinct population of $CD44^+$ cells with no detectable CD62L in the spleen (Fig. 6D and E). Moreover, the frequency of the Eff./EM $CD8^+$ T-cell populations was altered in the LN of the *Furin* cKO mice compared to the WT littermate animals ($p = 0.029$) (Fig. 6E). A similar aberrant CD62L "intermediate" pattern was also seen in older 5-month-old *Furin* cKO mice (data not shown). In conclusion, our data suggest that FURIN is required for the normal expression of genes associated with the TGFBR signaling pathway and the formation of memory $CD8^+$ T cells. Moreover, the lack of FURIN in the $CD8^+$ T cells alters the phenotype of the $CD44^+$ CTLs by modulating the expression of CD62L.

Discussion and conclusions

Despite the accumulating knowledge of the importance of FURIN in immunobiology, in infections and as a drug target, little is known about its impact on $CD8^+$ T cells. Here, we show that T-cell-specific *Furin* cKO mice have an attenuated early host response against an LCMV infection characterized by increased viral titers and decreased serum IFNG levels. Furthermore, the comprehensive characterization of the *Furin* KO $CD8^+$ T cells using RNA sequencing and flow cytometry demonstrate that the absence of FURIN associates with an activated phenotype characterized by the upregulated expression of *Tbx21*, *Irf4*, and *Il12rb1* in naïve cells and the increased frequencies of $CD44^+$, $CD69^+$, TNF^+, and $IFNG^+$ cells in the peripheral lymphoid organs of *Furin* cKO mice. In contrast, *in vitro* activated *Furin* KO $CD8^+$ T cells produced significantly lower levels of GZMB and TNF than control cells. We further demonstrate that the TCR-activated FURIN-deficient $CD8^+$ T cells can respond to IL12 and TGFB1 but exhibit a substantially altered transcriptional signature in comparison to WT CTLs. Finally, we describe that the absence of FURIN from the CD8+ T lymphocytes can influence the differentiation of memory cells, as suggested by the downregulation of the *Eomes*, *Foxo1*, and *Tcf7* transcription factor genes in the TGFB1-treated *Furin* KO CTLs as well as the aberrant expression of ITGAE and CD62L in $CD8^+$ T cells in *Furin* cKO mice.

Altered expression levels of FURIN have been associated with human malignancies including lung and skin cancers [5, 6] as well as with autoimmune diseases such as Sjögren's syndrome and rheumatoid arthritis [37, 38]. In fact, cell therapy where a combination of granulocyte-macrophage colony stimulating factor (GMCSF) cDNA and a shRNA construct against *FURIN* (Vigil, Gradalis) are transfected into autologous tumor cells is currently being evaluated in phase I-III clinical trials against human gyneco-

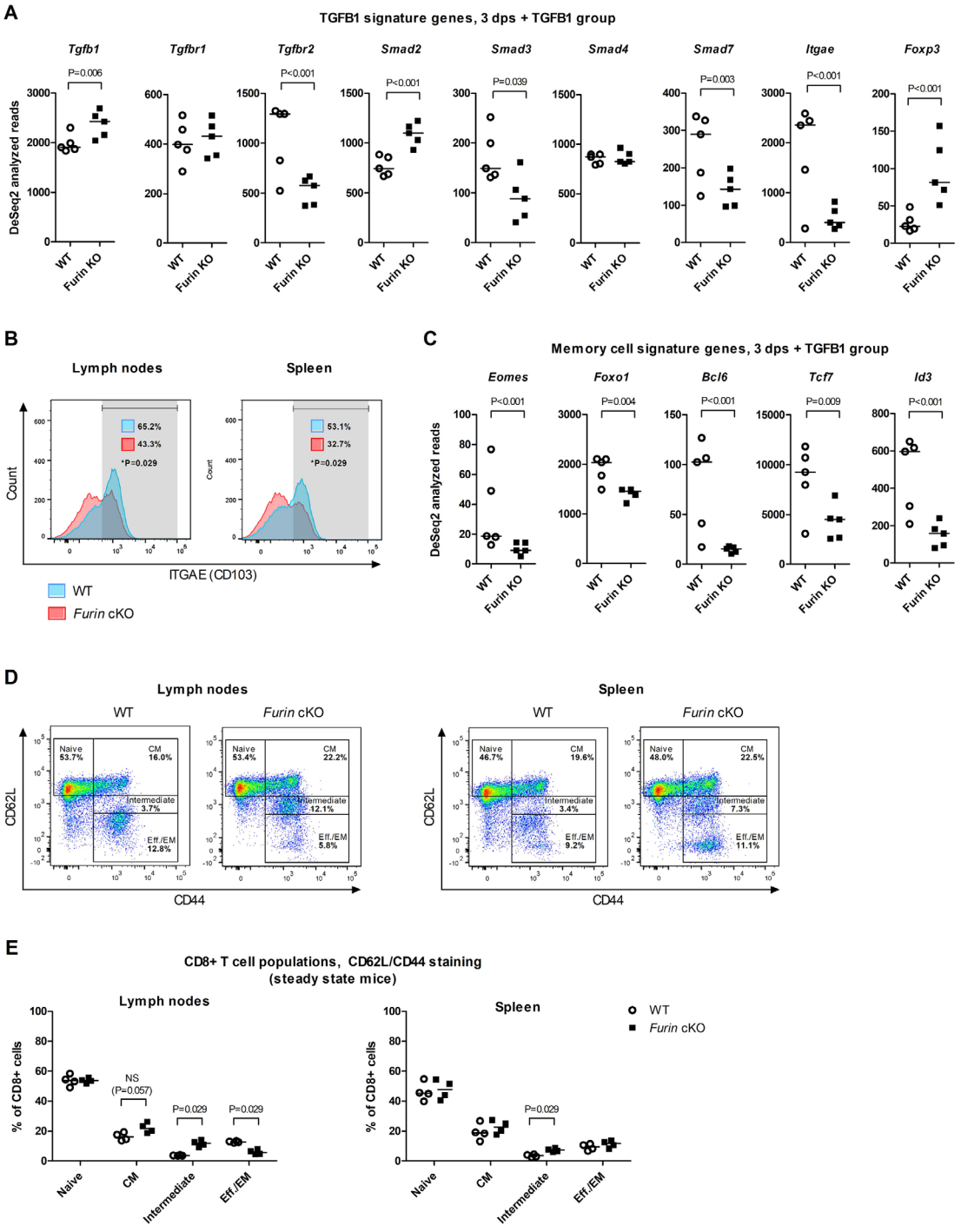

Figure 6. CD8$^+$ T-cell intrinsic FURIN is required for the normal expression of memory cell associated transcription factors and for normal CD8$^+$ T-cell memory cell frequencies. (A and C) Total RNA was isolated from the *in vitro* stimulated CD8$^+$ T cells, and a genome-wide gene expression analysis performed using RNA sequencing. In panel (A), the TCR-activated and TGFB1-treated *Furin* KO and WT cells were compared for the expression of genes associated with the TGFB1-signaling pathway, whereas in panel (C) genes related to CD8$^+$ memory T-cell development were compared. (B, D, and E) The LN and spleen cells from 3-month-old *Furin* cKO ($n = 4$, two females, two males) and WT mice ($n = 4$, two females, two males) were isolated and the surface expression of ITGAE, CD62L, and CD44 evaluated within the CD8$^+$ T-cell compartment using flow cytometry. In panel (B), the representative histograms of ITGAE$^+$ cells within the CD8$^+$ T cells are shown. In panel (D), the target populations were gated based on the expression of CD62L and CD44 and the representative flow cytometry plots are shown. In panels (B) and (D) 4800–5000 down-sampled cells were used from each sample and the concatenated FCS-files (19 200–20 000 cells/genotype) are depicted. The gates demonstrate the average frequency within a group. In panel (E), the frequencies of naïve, central memory (CM), "intermediate," and effector/effector memory (Eff./EM) populations of CD8$^+$ T cells are shown. The experiments in panels (A/C) and (B) were done once, whereas a representative of two experiments is shown in panels (D) and (E). In panels (A) and (C), the statistical evaluation of differences was done using DESeq2 and adjusted using the Benjamini–Hochberg method. A two-tailed Mann–Whitney test was used for the statistical comparison of differences in panels (B) and (D).

logical cancers and Ewing's sarcoma [39–41]. Importantly, FURIN also has broad immunological functions in modulating the production of antimicrobial peptides and cytokine secretion [9, 11–13, 42]. FURIN can activate bacterial toxins like Shiga and diphtheria as well as viral envelope proteins of the human immunodeficiency virus (HIV) and SARS-CoV-2 [2, 6, 7]. In fact, blocking FURIN activity has the potential of becoming a novel treatment for cancers and many infectious diseases as it enables modulation of the immune response as well as reduces bacterial and viral pathogenicity. In the current study, we infected *Furin* cKO mice with a pathogen that provokes the $CD8^+$ T-cell response, LCMV, and demonstrated that the lack of FURIN from T lymphocytes causes an inability to restrain viral loads and decreases the secretion of IFNG into the circulation at 5 dpi. Importantly, our results show that FURIN activity in T cells is required for the normal host response against a viral infection, which should be taken into consideration when assessing the use of FURIN blockade as a therapeutic approach. To improve understanding on how FURIN deficiency impacts the differentiation of the LCMV-specific CTLs and their function, further studies using MHC class I tetramers should be conducted. Furthermore, to exclude indirect effects of inherent autoimmunity that may impact $CD8^+$ T-cell differentiation in *Cd4-Cre-Furin*$^{flox/flox}$ animals, a chimeric setting containing WT and FURIN-deficient T-cell compartments or alternatively *Cd8-Cre-Furin*$^{flox/flox}$ animals would be important.

Out of the 32 DEGs between naïve *Furin* KO and control $CD8^+$ T cells, we identified the upregulation of important T-cell factors including *Tbx21*, *Irf4*, *Il12rb1*, and *Socs3* in the absence of FURIN. While TBX21 (also known as T-bet) was initially discovered as a transcription factor that polarizes naïve $CD4^+$ T cells into the Th1 subset [43], it was later shown that TBX21 also regulates the differentiation of effector $CD8^+$ T cells [44]. Similarly, IRF4 and IL12 signaling can promote the development and cytotoxicity of effector CTLs, as was demonstrated by the impaired abilities of *Irf4* and *Il12p35* KO CD8+ T cells to control *Listeria monocytogenes* and *Toxoplasma gondii* infections, respectively [45, 46]. Providing a negative feedback mechanism, SOCS3, a renowned regulator of the JAK/STAT signaling, can in turn inhibit the IL12-mediated activation of T cells [47]. Taken together, *Tbx21*, *Irf4*, *Il12rb1*, and *Socs3* intertwine into a gene expression network controlling the differentiation of effector CTLs, and their upregulation in naïve *Furin* KO $CD8^+$ T cells suggests an inherent, activated $CD8^+$ T-cell phenotype in the absence of intrinsically produced FURIN. The T-cell effector-like phenotype was not observed when the levels of FOXP3, IL2RA, and CD44 were evaluated in thymic SP $CD8^+$ T cells, which in turn implies that FURIN may regulate naïve T-cell activation after thymic egress in secondary lymphoid organs. However, the mechanisms by which FURIN impacts the naive T-cell phenotype remain elusive and a more detailed, developmental stage-specific characterization of immature double positive and SP $CD8^+$ thymocytes in *Furin* cKO animals is clearly warranted.

In the current study, we performed a detailed *ex vivo* characterization of *Furin* KO $CD8^+$ T cells using flow cytometry. The increased frequencies of $CD44^+$, $CD69^+$, and $IFNG^+$ cells within the $CD8^+$ T-cell compartment of *Furin* cKO mice are in line with our previous findings [11, 20]. In addition, we show a decreased percentage of $IL7RA^+$, and higher fractions of TNF^+ cells among the $CD8^+$ T cells supporting an activated phenotype. Importantly, the flow cytometric analysis in both 3- and 5-month-old mice provides new information on the temporality of the phenotype, and it is in line with our previous report on an age-related autoimmune response in the gut of the *Furin* cKO mice [11]. Interestingly, while inhibition of PD1 expression was previously reported in $CD8^+$ T cells treated with PCSK inhibitors [27], our results indicate that FURIN is dispensable for PD1 production in $CD8^+$ T cells. In order to corroborate the significance of the overtly activated *Furin* KO $CD8^+$ T cells in the pathogenesis of inflammatory bowel disease, a careful phenotypical and functional examination of the tissue resident $CD8^+$ T cells would be required, and further studies are needed to clarify the associations between different PCSK enzymes and PD1 in T cells.

The specific mechanisms for why the inherently upregulated CTL effector profile in *Furin* KO $CD8^+$ T cells is not translated into enhanced host responses against LCMV requires further studies. We have previously shown that FURIN regulates transcription factors involved in T-cell activation, including nuclear factor of activated T cells (NFAT) and nuclear factor NF-kappa-B subunit 1 (NFKB1), and that FURIN-mediated transactivation controls IL2 production upon TCR stimulation in mouse $CD4^+$ T cells and in human Jurkat T cells [21]. Quantification of effector proteins in the culture media of *in vitro* stimulated $CD8^+$ T cells revealed that FURIN restrains IL2 production upon activation but promotes the production of GZMB and TNF. Although the results of the anti-CD3/anti-CD28 antibody-activated CTLs and the LCMV infection should be compared with caution, the altered secretion of IL2, GZMB, and TNF as well as the downregulated viral defense genes such as *Bcl3*, *Ifit3*, and *Irf1* observed *in vitro* provide possible mechanistic explanations for the trend of higher $CD8^+$ T-cell counts in the LCMV-infected *Furin* cKO mice and their attenuated host response. Nevertheless, the divergent IFNG levels between the two experimental systems underscores the differences between the experimental set ups. For example, in LCMV-infected animals, several cell types contribute to the serum IFNG levels and only naïve CD8 cells were included in the *in vitro* activation experiments. To address the antigen-restricted cytotoxicity of the FURIN-deficient $CD8^+$ T cells in an antigen-dependent manner, we tried to cross our *Cd4-Cre-Furin*$^{flox/flox}$ mice together with the OT-1 mouse strain: C57BL/6-Tg(TcraTcrb)1100Mjb/Crl (Charles River, Massachusetts, USA). However, despite extensive efforts, we could not obtain mice carrying homozygous *Tcra/Tcrb* transgenes together with the *Cd4-Cre*-expressing allele nor any other suitable genotype combinations for our cytotoxicity analysis. Our failed efforts may arise from yet unidentified factors in combining the three different genetically engineered mouse strains. Future studies with alternative transgenic mouse strains, such as the LCMV gp33-specific P14 TCR animals, could potentially be beneficial in the evaluation of the antigen-restricted cytotoxicity of the FURIN-deficient $CD8^+$ T cells.

Delicate regulation of the transcriptome is essential for the CD8$^+$ T cells to respond appropriately to antigenic stimuli in the context of the tissue milieu [36]. TGFB1 is a pleiotropic cytokine that is important in a multitude of immunological processes such as lymphocyte development and the control of T-cell memory [48, 49]. More specifically, an infection with ovalbumin expressing *L. monocytogenes* in OT-1 transgenic mice revealed that the absence of functional TGFBR2 markedly decreased the frequency of the CD8$^+$ memory precursor effector cells and increased the amount of short-lived effector cells, and that the expression of the memory T-cell-associated markers EOMES, FOXO1, and BCL6 was reduced in the *Tgfbr2* KO CD8+ T cells compared to WT cells [32]. Additionally, FURIN is critical for the bioavailability of the mature TGFB1 cytokine, and serum contains substantial levels of active TGFB1. To evaluate which of the FURIN effects are mediated by TGFB1 activation, we used serum-free culture media and administered exogenous TGFB1 in its active form to the TCR-stimulated *Furin* KO CD8$^+$ T cells. The increased number of DEGs in these conditions argues that FURIN is important for the normal CTL response to TGFB1. For example, in the presence of TGFB1, the expression levels of TGFBR2-regulated and memory CD8$^+$ T-cell-associated genes, among them *Eomes*, *Foxo1*, and *Bcl6*, were decreased in the FURIN-deficient cells. The flow cytometric analysis of ITGAE (a marker for T_{RM} cells) as well as CD62L and CD44 co-stained CD8$^+$ T cells suggested that FURIN is involved in the regulation of memory cell populations. Specifically, the CD8$^+$ T-cell-expressed FURIN seems to regulate a process that has previously been proposed to involve segregation of CD8$^+$ T cells into subpopulations expressing differential levels of CD62L [50]. As FURIN is a protease, the RNA sequencing experiments do not provide direct evidence on its function at the molecular lever. Furthermore, it is possible that FURIN acts on different intracellular processes in resting versus activated T cells, which may lead to different outcomes. Direct proteomic approaches should be conducted with CTLs to identify the direct target molecules for FURIN. This would also enlight the sequence of events that lead to the observed *Furin* KO CD8$^+$ T-cell phenotypes.

In *Cd4-Cre-Furin*$^{flox/flox}$ mice, *Furin* becomes deleted in all dividing cells that express CD4 during their life span, including CD8$^+$ T cells, Th cells, and CD4$^+$ NKT cells. This clearly calls for a cautious interpretation of our findings as *Furin* KO CD8$^+$ T cells may become impacted by other FURIN-deficient cell types, especially Th cells. Consequently, further studies using CD8$^+$ T-cell-specific *Furin* deletion (*Cd8a-Cre-Furin*$^{flox/flox}$) in mice will be important to confirm the significance of FURIN in the biology of CTLs *in vivo*. Importantly, activating naïve CD8$^+$ T cells from WT C57BL/6JRj mice in the presence of a FURIN/PCSK inhibitor, CMK (10 μM concentration), could partially recapitulate the findings obtained with *Furin* KO CTLs, which supports a cell-intrinsic role of FURIN in CD8$^+$ T cells that is independent of the autoinflammatory phenotype of *Cd4-Cre-Furin*$^{flox/flox}$ animals [11].

Limitations of the study can be listed as follows: (1) Since *Cd4-Cre-Furin*$^{flox/flox}$ mice were used in the LCMV infection experiments, the impact of FURIN-deficient CD4$^+$ T cells on the viral titers and IFNG production cannot be ruled out. (2) The overtly activated phenotype seen in steady-state *Furin* KO CD8$^+$ T cells could be influenced indirectly by the reduced suppressive capacity of FURIN-deficient Tregs or aberrant Th cell populations. (3) The direct endoproteolytic targets of FURIN in CD8$^+$ T cells were not studied, and thus the detailed mechanisms by which FURIN regulates the gene expression in CTLs remain unclear. (4) *Cd4-Cre* animals (negative or heterozygous for *Furin*^{flox}-site) were not included as controls to evaluate the Cre-recombinase-mediated cytotoxicity.

Here, we demonstrate that T-cell-expressed FURIN is required for the normal anti-viral host response against an experimental LCMV infection in mice. Moreover, our *ex vivo* characterization of CD8$^+$ T cells suggests that FURIN is essential for restraining an age-dependent, inherent activation of CTLs in steady-state mice, and for the normal TCR-mediated production of effector proteins such as GZMB and TNF. Our data imply a novel FURIN-dependent mechanism of regulation of the effector to memory transition of CD8$^+$ T cells that is possibly influenced by dysfunctional TGFBR signaling and not by intrinsic TGFB1 production. Taken together, we found that FURIN sustains important traits of CD8$^+$ T cells associated with the host response, auto-immunity, and the development of immunological memory, and therefore special attention is warranted before considering FURIN inhibition as a therapeutic approach.

Materials and methods

Mice

Unchallenged mice were housed in the pathogen-free preclinical facilities of the University of Turku (Turku, Finland) and Tampere University (Tampere, Finland). For the LCMV infection experiments, mice were maintained at Brown University animal facilities. Note that 8-week to 5-month-old transgenic *Cd4-Cre-Furin*$^{flox/flox}$ mice [11] and their *Furin*$^{flox/flox}$ littermates in a C57BL/6 background as well as WT C57BL/6JRj mice were used in the study. The transgenic mice were genotyped with PCR using Cre-specific primers; F: 5'-GCTAAGGATGACTCTGGTCA-3' and R: 5'-CTAATCGCCATCTTCCAGCA-3', and primers for the *Furin* flox-sites; F: 5'-ATGCTCAAGGCCAGAAGATC-3' and R: 5'-AATCTGTTCCCTGCTGAGGA-3' [51].

LCMV infection

The LCMV infections were done according to previously established protocols [22, 52]. In brief, mice were infected by an intraperitoneal injection of 2.5×10^4 PFUs of the LCMV Armstrong clone E350 and monitored until 5 or 8 dpi. LCMV loads in the spleen were quantified using NIH-3T3 cells in a standard plaque assay. To determine IFNG levels in the LCMV-infected mice, animals were euthanized and serum samples as well as tissue homogenates from the spleens were analyzed using ELISA.

Enumeration of $CD4^+$ and $CD8^+$ T cells upon LCMV infection was done using flow cytometry.

Cell purification

Lymph nodes (LNs) and spleen from *Cd4-Cre-Furin*$^{flox/flox}$ mice and their *Furin*$^{flox/flox}$ littermates as well as from WT C57BL/6JRj were isolated and single cell suspensions prepared by filtering the cells through a 70 μm Corning strainers (Sigma-Aldrich, Missouri, USA). Splenocytes were subsequently treated with 2 mL of ACK lysis buffer (Gibco/Thermo Fisher Scientific, Massachusetts, USA) to disrupt erythrocytes. Cells were kept on ice or at +4°C throughout the isolation procedure. Purification of naïve $CD8^+$ T cells for RNA sequencing was performed at the Cell Imaging and Cytometry Core of Turku Bioscience (University of Turku and Åbo Akademi University, Turku, Finland). In order to obtain a level of high purity for the cells for this analysis, total $CD8^+$ lymphocytes were first enriched using a mouse $CD8^+$ T-cell negative selection kit (#130-104-075, Miltenyi Biotec, Bergisch Gladbach, Germany) and MACS, which was followed by FACS using FACSAria Fusion (Becton, Dickinson and Company, NJ, USA) and fluorochrome-conjugated antibodies CD3-PerCP-eFluor710, CD8a-PE, CD62L-APC, and CD44-FITC (Becton, Dickinson and Company; Thermo Fisher Scientific). Sorted naïve $CD8^+$ T cells were resuspended in RLT buffer (Qiagen, Hilden, Germany) for RNA isolation. For the *in vitro* stimulation experiments, isolation of naïve $CD8^+$ T cells was performed following the manufacturer's instructions using a naive $CD8a^+$ T-cell isolation kit (#130-096-543, Miltenyi Biotec) and MACS.

Flow cytometry

Isolated cell suspensions were stained with the FVS510 viability stain (Becton, Dickinson and Company) and Fc-receptors blocked using a CD16/CD32 Monoclonal Antibody (Thermo Fisher Scientific, Massachusetts, US; Becton, Dickinson and Company) followed by incubation with fluorescently labeled anti-mouse antibodies CD3-FITC, CD8a-PerCP-Cy5.5, CD44-APC-Cy7, CD69-APC, PD1-SuperBright780, IL7RA-eFluor450, FASL-SuperBright600, TNF-PE-Cy7, IFNG-PE-Cy7, ITGAE-BV786, and CD62L-eFluor450 (Becton, Dickinson and Company; Thermo Fisher Scientific). For intracellular staining of the $CD8^+$ T cells, the cells were treated with phorbol 12-myristate 13-acetate (PMA, 50 ng/mL) (Sigma-Aldrich), calcium ionophore (1 μg/mL) (Sigma-Aldrich), GolgiPlug (1.0 μL/mL) (Becton, Dickinson and Company) and GolgiStop (0.7 μL/mL) (Becton, Dickinson and Company) and incubated in 1 mL of RPMI-1640 media (Lonza, Basel, Switzerland) supplemented with 10% FBS (Gibco/Thermo Fisher Scientific), 1% penicillin-streptomycin (Lonza), 1% L-glutamine (Lonza), and 2-ME (50 μM) for 4 h at 37°C. Flow cytometry was done with FACSCanto or FACSAria Fusion (Becton, Dickinson and Company). For setting-up the compensation, individually stained primary cells, an anti-rat and anti-hamster Igκ/negative control compensation particles set (Becton, Dickinson and Company), and UltraComp eBeads (Thermo Fisher Scientific) were used. The guidelines for the use of flow cytometry and cell sorting in immunological studies were followed [53].

Mouse primary $CD8^+$ T-cell culture

Note that 24-well cell culture plates were prepared by overnight incubation with an anti-CD3 monoclonal antibody (17A2; 5 μg/mL) (eBioscience/Thermo Fisher Scientific) and an anti-CD28 monoclonal antibody (37.51; 5 μg/mL) (eBioscience/Thermo Fisher Scientific) at +4°C. The naïve $CD8^+$ T cells were applied onto the anti-CD3/anti-CD28-coated plates using 0.5–1.2 × 10^6 cells/well and incubated in 1 mL of X-VIVO 20 Serum-free Hematopoietic Cell Medium (Lonza) for 3 days at 37°C without added cytokines or in the presence of recombinant IL12 (10 ng/mL) (Peprotech, NJ, USA) or TGFB1 (0.5 ng/mL) (Peprotech). In the FURIN/PCSK inhibitor experiment, a 10 mM stock of decanoyl-RVKR-chloromethylketone (CMK) (Sigma-Aldrich) was prepared in DMSO (Sigma-Aldrich), and the stock solution was administered onto the wells to obtain 10 μM (0.1% DMSO) and 30 μM (0.3% DMSO) concentrations of the inhibitor during the T-cell activation. After a 3-day stimulation, the $CD8^+$ T cells were collected into RLT buffer (Qiagen) for RNA isolation and mRNA quantification. IL2, GZMB, IFNG, and TNF concentrations in the culture media were quantified using mouse uncoated ELISA kits (Thermo Fisher Scientific) following the manufacturer's instructions.

RNA sequencing

RNA isolation was performed according to the manufacturer's instructions using the RNeasy Mini Kit or RNeasy Plus Mini Kit (Qiagen). The naïve $CD8^+$ T-cell RNA sequencing was done at the Finnish Functional Genomics Centre of Turku Bioscience (University of Turku), whereas the RNA sequencing of stimulated $CD8^+$ T cells was performed at the Functional Genomics Unit of the HiLIFE Genome Analysis Infrastructure (University of Helsinki, Helsinki, Finland). A FASTQ data quality analysis and alignment to the mouse reference genome, GRCm38.p6 (Genome Reference Consortium), were done with Snakemake (v. 5.6.0) [54]. Reads were mapped with the Spliced Transcripts Alignment to a Reference (STAR) wrapper, providing an ENSEMBL release 97 reference and annotations for gene count quantification. Differential gene expression analyses were performed with the R-software (v. 3.6.0) using DESeq2 (v. 1.24.0) [55] and annotated with biomaRt (v. 2.40.5) [56]. Transcripts with Benjamini–Hochberg adjusted $p < 0.05$ [57] were considered differentially expressed and chosen for further analysis. The regularized log (rlog)-transformed gene counts were visualized with pheatmap [58] and the Prism program (v. 5.02, GraphPad Software, Inc., CA, USA). To estimate the efficiency of the genomic *Furin* deletion, the exon-level counts for aligned reads were quantified with subread 2.0.0 featureCounts

[59]. Moreover, Integrative Genomics Viewer was used for a visual inspection of the aligned reads focusing on exon2 [60].

Statistical analysis

Group sizes were based on previous experimental observations. Statistical analyses of the RNA sequencing have been described above. For other parts, statistics were performed using a nonparametric two-tailed Mann–Whitney and the Prism program (v. 5.02, GraphPad Software). *p*-values of less than 0.05 were consider statistically significant.

Acknowledgements: This work is dedicated to the memory of Christine Biron. We thank the preclinical facility of Tampere University, partly funded by Biocenter Finland, and the preclinical facility of University of Turku for maintaining and providing us with the mice. We also thank Finnish Cell Imaging and Cytometry Centre supported by University of Turku, Åbo Akademi University and Biocenter Finland as well as Biomedicum Functional Genomics Unit at the Helsinki Institute of Life Science and Biocenter Finland at the University of Helsinki. The authors additionally acknowledge the Tampere facility of Flow Cytometry for their service. We especially thank many of our co-workers for technical assistance and scientific advice. We are grateful for Helen Cooper for proof-reading the manuscript. This study was financially supported by the Academy of Finland (Grant Nos. 295814 to M.J.T.O./Ma.P., 25013080481 and 25013142041 to I.S.J.), the Cancer Foundation of Finland (Grant Nos. 180138 to Ma.P.; 190146 to M.J.T.O./Ma.P.), the Paulo Foundation (M.J.T.O.), Tampere ImmunoExcellence-Vaccines and Immunomodulation Platform (M.J.T.O.), the Competitive State Research Financing of the Expert Responsibility Area of Tampere University Hospital/ Fimlab Laboratories (Grant Nos. X50070 to Ma.P.; X51409 to I.S.J., 9X011 and 9V010 to T.A.H.J.), Tampere University Hospital Support Foundation (I.S.J.), Päivikki and Sakari Sohlberg Foundation (T.A.H.J.), and Tampere Tuberculosis Foundation (M.J.T.O., T.A.H.J., and I.S.J.). The funding parties were not involved in the study design, in the collection, analysis or interpretation of the data, in the writing of the report or in the decision to submit the article for publication. The graphical abstract was created with BioRender.com.

Conflicts of interest: The authors declare no financial or commercial conflicts of interest.

Author contributions: M.J.T.O., M.N., I.S.J., T.A.H.J., J.J.O´S., C.A.B., and Ma.P. provided materials, funding, and facilities for the research. M.J.T.O., M.N., J.K., M.V., I.S.J., T.A.H.J., J.J.O´S., C.A.B., and Ma.P. designed and/or directed the experiments. M.J.T.O., F.M.C., S.A., M.J.P., Z.O., Me.P., M.V., and J.M. performed the experiments. M.J.T.O., F.M.C., Me.P., and J.M. analyzed the data. M.J.T.O. and Ma.P. wrote the paper. All authors reviewed and approved the manuscript.

Ethics approval: The mouse maintenance and the experiments were done according to the EU Directive (2010/63/EU) guidelines and the Finnish Act on the Protection of Animals Used for Scientific or Educational Purposes (497/2013). The experiments were approved by the Animal Experiment Board of Finland (permit: ESAVI/6781/2018), and the Reporting of In Vivo Experiments (ARRIVE) guidelines were followed. LCMV infection experiments were done according to the National Institutes of Health (NIH) guidelines and animal permits.

Data availability statement: RNA sequencing data has been submitted to the Gene Expression Omnibus (GEO) repository (identifier code: GSE186813). Other generated and analyzed data are available on reasonable request from the corresponding author.

Peer review: The peer review history for this article is available at https://publons.com/publon/10.1002/eji.202250246

References

1 **Fuller, R. S.**, **Brake, A. J.** and **Thorner, J.**, Intracellular targeting and structural conservation of a prohormone-processing endoprotease. *Science* 1989. **246**: 482–486.

2 **Thomas, G.**, Furin at the cutting edge: from protein traffic to embryogenesis and disease. *Nat. Rev. Mol. Cell Biol.* 2002. **3**: 753–766.

3 **Turpeinen, H.**, **Ortutay, Z.** and **Pesu, M.**, Genetics of the first seven proprotein convertase enzymes in health and disease. *Curr. Genomics* 2013. **14**: 453–467.

4 **Seidah, N. G.** and **Prat, A.**, The biology and therapeutic targeting of the proprotein convertases. *Nat. Rev. Drug Discovery* 2012. **11**: 367–383.

5 **Siegfried, G.**, **Descarpentrie, J.**, **Evrard, S.** and **Khatib, A.-M.**, Proprotein convertases: key players in inflammation-related malignancies and metastasis. *Cancer Lett.* 2020. **473**: 50–61.

6 **Braun, E.** and **Sauter, D.**, Furin-mediated protein processing in infectious diseases and cancer. *Clin. Transl. Immunol.* 2019. **8**: e1073.

7 **Xia, S.**, **Lan, Q.**, **Su, S.**, **Wang, X.**, **Xu, W.**, **Liu, Z.**, **Zhu, Y.** et al., The role of furin cleavage site in SARS-CoV-2 spike protein-mediated membrane fusion in the presence or absence of trypsin. *Signal Transduction Targeted Ther.* 2020. **5**: 1–3.

8 **Johnson, B. A.**, **Xie, X.**, **Bailey, A. L.**, **Kalveram, B.**, **Lokugamage, K. G.**, **Muruato, A.**, **Zou, J.** et al., Loss of furin cleavage site attenuates SARS-CoV-2 pathogenesis. *Nature* 2021. **591**: 293–299.

9 **Pesu, M.**, **Muul, L.**, **Kanno, Y.** and **O'Shea, J. J.**, Proprotein convertase furin is preferentially expressed in T helper 1 cells and regulates interferon gamma. *Blood* 2006. **108**: 983–985.

10 **Lund, R. J.**, **Chen, Z.**, **Scheinin, J.** and **Lahesmaa, R.**, Early target genes of IL-12 and STAT4 signaling in the cells. *J. Immunol.* 2004. **172**: 6775–6782.

11 **Pesu, M.**, **Watford, W. T.**, **Wei, L.**, **Xu, L.**, **Fuss, I.**, **Strober, W.**, **Andersson, J.** et al., T-cell-expressed proprotein convertase furin is essential for maintenance of peripheral immune tolerance. *Nature* 2008. **455**: 246–250.

12 **Oksanen, A.**, **Aittomäki, S.**, **Jankovic, D.**, **Ortutay, Z.**, **Pulkkinen, K.**, **Hämäläinen, S.**, **Rokka, A.** et al., Proprotein convertase FURIN constrains Th2 differentiation and is critical for host resistance against *Toxoplasma gondii*. *J. Immunol.* 2014. **193**: 5470–5479.

13 **Cordova, Z. M.**, **Grönholm, A.**, **Kytölä, V.**, **Taverniti, V.**, **Hämäläinen, S.**, **Aittomäki, S.**, **Niininen, W.** et al., Myeloid cell expressed proprotein convertase FURIN attenuates inflammation. *OncoTargets Ther.* 2016. **7**: 54392–54404.

14 **Ojanen, M. J. T.**, **Turpeinen, H.**, **Cordova, Z. M.**, **Hammarén, M. M.**, **Harjula, S.-K. E.**, **Parikka, M.**, **Rämet, M.** et al., The proprotein convertase subtilisin/kexin furinA regulates zebrafish host response against *Mycobacterium marinum*. *Infect. Immun.* 2015. **83**: 1431–1442.

15 **Aittomäki, S.**, **Valanne, S.**, **Lehtinen, T.**, **Matikainen, S.**, **Nyman, T. A.**, **Rämet, M.** and **Pesu, M.**, Proprotein convertase Furin1 expression in the Drosophila fat body is essential for a normal antimicrobial peptide response and bacterial host defense. *FASEB J.* 2017. **31**: 4770–4782.

16 **Dubois, C. M.**, **Blanchette, F.**, **Laprise, M. H.**, **Leduc, R.**, **Grondin, F.** and **Seidah, N. G.**, Evidence that furin is an authentic transforming growth factor-beta1-converting enzyme. *Am. J. Pathol.* 2001. **158**: 305–316.

17 **Farhood, B.**, **Najafi, M.** and **Mortezaee, K.**, CD8+ cytotoxic T lymphocytes in cancer immunotherapy: a review. *J. Cell. Physiol.* 2019. **234**: 8509–8521.

18 **Halle, S.**, **Halle, O.** and **Förster, R.**, Mechanisms and dynamics of T cell-mediated cytotoxicity in vivo. *Trends Immunol.* 2017. **38**: 432–443.

19 **He, Z.**, **Khatib, A.-M.** and **Creemers, J. W. M.**, Loss of the proprotein convertase Furin in T cells represses mammary tumorigenesis in oncogene-driven triple negative breast cancer. *Cancer Lett.* 2020. **484**: 40–49.

20 **Vähätupa, M.**, **Aittomäki, S.**, **Cordova, Z. M.**, **May, U.**, **Prince, S.**, **Uusitalo-Järvinen, H.**, **Järvinen, T. A.** et al., T-cell-expressed proprotein convertase FURIN inhibits DMBA/TPA-induced skin cancer development. *Oncoimmunology* 2016. **5**: e1245266.

21 **Ortutay, Z.**, **Oksanen, A.**, **Aittomäki, S.**, **Ortutay, C.** and **Pesu, M.**, Proprotein convertase FURIN regulates T cell receptor-induced transactivation. *J. Leukocyte Biol.* 2015. **98**: 73–83.

22 **Orange, J. S.**, **Wolf, S. F.** and **Biron, C. A.**, Effects of IL-12 on the response and susceptibility to experimental viral infections. *J. Immunol.* 1994. **152**: 1253–1264.

23 **Bhat, P.**, **Leggatt, G.**, **Waterhouse, N.** and **Frazer, I. H.**, Interferon-γ derived from cytotoxic lymphocytes directly enhances their motility and cytotoxicity. *Cell Death. Dis.* 2017. **8**: e2836.

24 **Butz, E. A.** and **Bevan, M. J.**, Massive expansion of antigen-specific CD8+ T cells during an acute virus infection. *Immunity* 1998. **8**: 167–175.

25 **Su, H. C.**, **Cousens, L. P.**, **Fast, L. D.**, **Slifka, M. K.**, **Bungiro, R. D.**, **Ahmed, R.** and **Biron, C. A.**, CD4+ and CD8+ T cell interactions in IFN-gamma and IL-4 responses to viral infections: requirements for IL-2. *J. Immunol.* 1998. **160**: 5007–5017.

26 **Cheng, Y.-W.**, **Chao, T.-L.**, **Li, C.-L.**, **Chiu, M.-F.**, **Kao, H.-C.**, **Wang, S.-H.**, **Pang, Y.-H.** et al., Furin inhibitors block SARS-CoV-2 spike protein cleavage to suppress virus production and cytopathic effects. *Cell Rep.* 2020. **33**: 108254.

27 **Tomé, M.**, **Pappalardo, A.**, **Soulet, F.**, **López, J. J.**, **Olaizola, J.**, **Leger, Y.**, **Dubreuil, M.** et al., Inactivation of proprotein convertases in T cells inhibits PD-1 expression and creates a favorable immune microenvironment in colorectal cancer. *Cancer Res.* 2019. **79**: 5008–5021.

28 **Eden, E.**, **Navon, R.**, **Steinfeld, I.**, **Lipson, D.** and **Yakhini, Z.**, GOrilla: a tool for discovery and visualization of enriched GO terms in ranked gene lists. *BMC Bioinf.* 2009. **10**: 48.

29 **Duckert, P.**, **Brunak, S.** and **Blom, N.**, Prediction of proprotein convertase cleavage sites. *Protein Eng. Des. Sel.* 2004. **17**: 107–112.

30 **Schjoldager, K. T.-B. G.**, **Vester-Christensen, M. B.**, **Goth, C. K.**, **Petersen, T. N.**, **Brunak, S.**, **Bennett, E. P.**, **Levery, S. B.** et al., A systematic study of site-specific GalNAc-type O-glycosylation modulating proprotein convertase processing. *J. Biol. Chem.* 2011. **286**: 40122–40132.

31 **de Zoeten, E. F.**, **Lee, I.**, **Wang, L.**, **Chen, C.**, **Ge, G.**, **Wells, A. D.**, **Hancock, W. W.** et al., Foxp3 processing by proprotein convertases and control of regulatory T cell function. *J. Biol. Chem.* 2009. **284**: 5709–5716.

32 **Ma, C.** and **Zhang, N.**, Transforming growth factor-β signaling is constantly shaping memory T-cell population. *Proc. Nat. Acad. Sci. USA* 2015. **112**: 11013–11017.

33 **Corgnac, S.**, **Boutet, M.**, **Kfoury, M.**, **Naltet, C.** and **Mami-Chouaib, F.**, The emerging role of CD8+ tissue resident memory T (TRM) cells in antitumor immunity: a unique functional contribution of the CD103 integrin. *Front. Immunol.* 2018. **9**: 1904.

34 **Mokrani, M.**, **Klibi, J.**, **Bluteau, D.**, **Bismuth, G.** and **Mami-Chouaib, F.**, Smad and NFAT pathways cooperate to induce CD103 expression in human CD8 T lymphocytes. *J. Immunol.* 2014. **192**: 2471–2479.

35 **Mami-Chouaib, F.** and **Tartour, E.**, Editorial: tissue resident memory T cells. *Front. Immunol.* 2019. **10**: 1018.

36 **Kaech, S. M.** and **Cui, W.**, Transcriptional control of effector and memory CD8+ T cell differentiation. *Nat. Rev. Immunol.* 2012. **12**: 749–761.

37 **Valli, A.**, **Ranta, N.**, **Grönholm, A.**, **Silvennoinen, O.**, **Pesu, M.** and **Isomäki, P.**, Increased expression of the proprotein convertase enzyme FURIN in rheumatoid arthritis. *Scand. J. Rheumatol.* 2019. **48**: 173–177.

38 **Ranta, N.**, **Valli, A.**, **Grönholm, A.**, **Silvennoinen, O.**, **Isomäki, P.**, **Pesu, M.** and **Pertovaara, M.**, Proprotein convertase enzyme FURIN is upregulated in primary Sjögren's syndrome. *Clin. Exp. Rheumatol.* 2018. **36**: 47–50.

39 **Rocconi, R. P.**, **Grosen, E. A.**, **Ghamande, S. A.**, **Chan, J. K.**, **Barve, M. A.**, **Oh, J.**, **Tewari, D.** et al., Gemogenovatucel-T (Vigil) immunotherapy as maintenance in frontline stage III/IV ovarian cancer (VITAL): a randomised, double-blind, placebo-controlled, phase 2b trial. *Lancet Oncol.* 2020. **21**: 1661–1672.

40 **Senzer, N.**, **Barve, M.**, **Kuhn, J.**, **Melnyk, A.**, **Beitsch, P.**, **Lazar, M.**, **Lifshitz, S.** et al., Phase I trial of "bi-shRNAifurin/GMCSF DNA/autologous tumor cell" vaccine (FANG) in advanced cancer. *Mol. Ther.* 2012. **20**: 679–686.

41 **Ghisoli, M.**, **Barve, M.**, **Schneider, R.**, **Mennel, R.**, **Lenarsky, C.**, **Wallraven, G.**, **Pappen, B. O.** et al., Pilot trial of FANG immunotherapy in Ewing's sarcoma. *Mol. Ther.* 2015. **23**: 1103–1109.

42 **Ortutay, Z.**, **Grönholm, A.**, **Laitinen, M.**, **Keresztes-Andrei, M.**, **Hermelo, I.** and **Pesu, M.**, Identification of novel genetic regulatory region for proprotein convertase FURIN and interferon gamma in T cells. *Front. Immunol.* 2021. **12**: 630389.

43 **Szabo, S. J.**, **Kim, S. T.**, **Costa, G. L.**, **Zhang, X.**, **Fathman, C. G.** and **Glimcher, L. H.**, A novel transcription factor, T-bet, directs Th1 lineage commitment. *Cell* 2000. **100**: 655–669.

44 **Sullivan, B. M.**, **Juedes, A.**, **Szabo, S. J.**, **von Herrath, M.** and **Glimcher, L. H.**, Antigen-driven effector CD8 T cell function regulated by T-bet. *Proc. Nat. Acad. Sci. USA* 2003. **100**: 15818–15823.

45 **Raczkowski, F.**, **Ritter, J.**, **Heesch, K.**, **Schumacher, V.**, **Guralnik, A.**, **Höcker, L.**, **Raifer, H.** et al., The transcription factor interferon regulatory factor 4 is required for the generation of protective effector CD8+ T cells. *Proc. Nat. Acad. Sci. USA* 2013. **110**: 15019–15024.

46 **Wilson, D. C.**, **Matthews, S.** and **Yap, G. S.**, IL-12 signaling drives CD8+ T cell IFN-gamma production and differentiation of KLRG1+ effector subpopulations during *Toxoplasma gondii* Infection. *J. Immunol.* 2008. **180**: 5935–5945.

47 **Yamamoto, K.**, **Yamaguchi, M.**, **Miyasaka, N.** and **Miura, O.**, SOCS-3 inhibits IL-12-induced STAT4 activation by binding through its SH2

domain to the STAT4 docking site in the IL-12 receptor beta2 subunit. *Biochem. Biophys. Res. Commun.* 2003. **310**: 1188–1193.

48 **Li, M. O.** and **Flavell, R. A.**, TGF-beta: a master of all T cell trades. *Cell* 2008. **134**: 392–404.

49 **Takai, S.**, **Schlom, J.**, **Tucker, J.**, **Tsang, K. Y.** and **Greiner, J. W.**, Inhibition of TGF-β1 signaling promotes central memory T cell differentiation. *J. Immunol.* 2013. **191**: 2299–2307.

50 **Kinjyo, I.**, **Qin, J.**, **Tan, S.-Y.**, **Wellard, C. J.**, **Mrass, P.**, **Ritchie, W.**, **Doi, A.** et al., Real-time tracking of cell cycle progression during CD8+ effector and memory T-cell differentiation. *Nat. Commun.* 2015. **6**: 6301.

51 **Roebroek, A. J. M.**, **Taylor, N. A.**, **Louagie, E.**, **Pauli, I.**, **Smeijers, L.**, **Snellinx, A.**, **Lauwers, A.** et al., Limited redundancy of the proprotein convertase furin in mouse liver. *J. Biol. Chem.* 2004. **279**: 53442–53450.

52 **Orange, J. S.**, **Salazar-Mather, T. P.**, **Opal, S. M.**, **Spencer, R. L.**, **Miller, A. H.**, **McEwen, B. S.** and **Biron, C. A.**, Mechanism of interleukin 12-mediated toxicities during experimental viral infections: role of tumor necrosis factor and glucocorticoids. *J. Exp. Med.* 1995. **181**: 901–914.

53 **Cossarizza, A.**, **Chang, H.-D.**, **Radbruch, A.**, **Abrignani, S.**, **Addo, R.**, **Akdis, M.** et al., Guidelines for the use of flow cytometry and cell sorting in immunological studies (third edition). *Eur. J. Immunol.* 2021. **51**: 2708–3145.

54 **Köster, J.** and **Rahmann, S.**, Snakemake—a scalable bioinformatics workflow engine. *Bioinformatics* 2012. **28**: 2520–2522.

55 **Love, M. I.**, **Huber, W.** and **Anders, S.**, Moderated estimation of fold change and dispersion for RNA-seq data with DESeq2. *Genome Biol.* 2014. **15**: 550.

56 **Durinck, S.**, **Spellman, P. T.**, **Birney, E.** and **Huber, W.**, Mapping identifiers for the integration of genomic datasets with the R/Bioconductor package biomaRt. *Nat. Protoc.* 2009. **4**: 1184–1191.

57 **Benjamini, Y.** and **Hochberg, Y.**, Controlling the false discovery rate: a practical and powerful approach to multiple testing. *J. R. Stat. Soc., B: Stat. Methodol.* 1995. **57**: 289–300.

58 **Raivo, K.**, R. pheatmap: Pretty heatmaps. 2019.

59 **Liao, Y.**, **Smyth, G. K.** and **Shi, W.**, featureCounts: an efficient general purpose program for assigning sequence reads to genomic features. *Bioinformatics*. 2014. **30**: 923–930.

60 **Robinson, J. T.**, **Thorvaldsdóttir, H.**, **Winckler, W.**, **Guttman, M.**, **Lander, E. S.**, **Getz, G.** and **Mesirov, J. P.**, Integrative genomics viewer. *Nat. Biotechnol.* 2011. **29**: 24–26.

Abbreviations: **cKO**: conditional KO · **DEG**: differentially expressed gene · **Eff./EM**: effector/effector memory · **FASL**: Fas ligand · **GO**: gene ontology · **GZMB**: granzyme B · **LCMV**: lymphocytic choriomeningitis virus · **PCSK**: proprotein convertase subtilisin/kexin · **PD1**: programmed cell death protein 1 · **PRF1**: perforin 1 · **SARS-CoV-2**: severe acute respiratory syndrome coronavirus 2 · **SP**: single positive · **TCR**: T-cell receptor · **TGFB1**: transforming growth factor beta-1

Full correspondence: Dr. Markus J.T. Ojanen, Faculty of Medicine and Health Technology, Tampere University, Arvo Ylpön katu 34, FI-33520 Tampere, Finland
e-mail: markus.ojanen@tuni.fi

Current address: Marko Pesu, Gilead Sciences Finland Oy, Karhumäentie 3, FI-01530 Vantaa, Finland.

Received: 27/10/2022
Revised: 16/3/2023
Accepted: 3/4/2023
Accepted article online: 4/4/2023